This is an open access article published under a Creative Commons Attribution (CC-BY) License, which permits unrestricted use, distribution and reproduction in any medium, provided the author and source are cited.

ACS AUTHORCHOICE

JOC The Journal of Organic Chemistry

pubs.acs.org/joc Article

Dynamic Induction of Optical Activity in Triarylmethanols and Their Carbocations

Bartosz Stasiak,* Agnieszka Czapik, and Marcin Kwit*

Cite This: J. Org. Chem. 2021, 86, 643−656 Read Online

ACCESS | Metrics & More | Article Recommendations | Supporting Information

ABSTRACT: A series of artificial triarylmethanols has been synthesized and studied toward the possibility of exhibiting an induced optical activity. The observed chiroptical response of these compounds resulted from the chiral conformation of a triarylmethyl core. The chirality induction from a permanent chirality element to the liable triarylmethyl core proceeds as a cooperative and cascade process. The OH···O(R) and/or (H)O···H_{ortho}C hydrogen bond formation along with the C−H···π interactions seem to be the most important factors that control efficiency of the chirality induction. The position of chiral and methoxy electron-donating groups within a trityl skeleton affects the amplitude of observed Cotton effects and stability of the trityl carbocations. In the neutral environment, the most intense Cotton effects are observed for *ortho*-substituted derivatives, which undergo a rapid decomposition associated with the complete decay of ECD signals upon acidification. From all of the in situ generated stable carbocations, only two exhibit intense Cotton effects in the low energy region at around 450 nm. The formation of carbocations is reversible; after alkalization, the ions return to the original neutral forms. Unlike most triarylmethyl derivatives known so far, in the crystal, the triarylmethanol, *para*-substituted with the chiral moiety, shows a propensity for a solid-state sorting phenomenon.

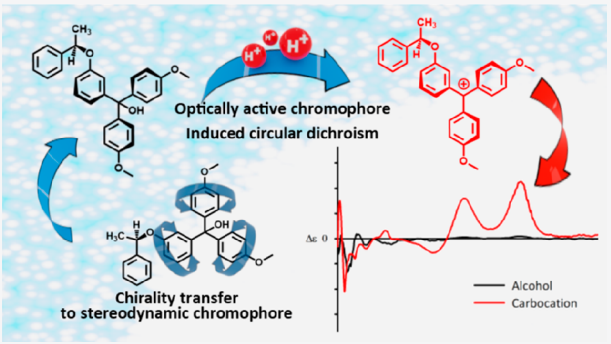

INTRODUCTION

The exceptional structural features and a wide-scope of applications make triphenylmethane (TrH), and related compounds of the general Ar_3X formula, interesting and still intensively explored objects of study. Besides being able to protect a polar functional group and supramolecular synthons, the presence of trityl(s) in a given molecular system is utilized in molecular tectonics for construction of the 3D networks and is crucial for the effective operation of some molecular devices.[1−3] The trityl-containing amino acids are promising candidates for the lead structures in medicinal chemistry.[4] The tritylium ion, one of the first ever discovered, was recognized for ages as an isolated curiosity of chemistry.[5] Now, the tritylium (triarylium) ions are employed as Lewis acid in synthesis, including catalytic stereoselective transfomations.[6] While early attempts to employ asymmetric catalysis with the use of optically active carbocations provided unsatisfactory results in terms of enantioselectivity, recent studies have indicated an advantage of latent trityl cations in the catalytic reactions.[7−9]

Apart from applications in synthesis, the pioneering works of Mislow and Iwamura on the triaryl molecular propellers, exhibiting so-called residual stereochemistry, are considered one of the foundations of dynamic stereochemistry.[10,11] In the parent TrH, the aryl rings adapt the twisted C_3-symmetrical conformation of either *P* or *M* helicity, dynamically transforming into one another; hence, neither trityl nor its ionized forms are optically active.[12] The induction of an optical activity revealed in the appearance of non-zero Cotton effects (CEs) in electronic circular dichroism (ECD) is achieved by linking chiral substituents to the central sp^3-hybridized carbon atom. Adaptation of trityl to the structure of chiral secondary alcohols, through the bevel-gear mechanism, was demonstrated for the first time by Gawronski.[13] Since then, a process of chirality transmission from the permanent chirality element to the stereodynamic trityl has been exploited by us and others for stereochemical assignments of alcohols, amines, sulfides, and selenides.[14] For all systems studied so far, the final, observed effects have provided evidence for a dynamic induction of the optical activity,[15] the detailed mechanism of the chirality transfer phenomenon is rather case sensitive.

In contrast to the trityl radicals, the chiroptical properties of tritylium cations have not been yet the subject of an in-depth study.[16−18] This remains rather an unexpected conclusion

Received: September 25, 2020
Published: December 22, 2020

ACS Publications © 2020 American Chemical Society

https://dx.doi.org/10.1021/acs.joc.0c02289
J. Org. Chem. 2021, 86, 643−656

when one takes into account the significance of tritylium (and related) cations in chemistry and, especially, the growing importance of these compounds in stereoselective synthesis and in material chemistry. Recently, Suzuki and co-workers have reported systems based on biphenyl-2,2′-diyl-type dicationic dyes as those exhibiting strong chiroptical signals.[19] However, it can be supposed that the optical activity of dication was due to the hindered rotation around the aryl−aryl bond rather than to the specific helicity of the trityl fragments. Hence, this and related molecules cannot be regarded as systems dynamically adapting to the chiral environment.

RESULTS AND DISCUSSION

As has been mentioned above, the importance of trityls and trityliums in various aspects of chemistry is not related to the growing interest in their dynamic stereochemistry. In fact, this is somewhat understandable due to the complexity of the problems to be solved. Therefore, continuing our interest in the dynamic stereochemistry of chiral compounds, we have decided to expand our study on triarylmethyl systems that may exhibit an induced optical activity in the neutral and in the cationic form. The systems planned to study should constitute latent tritylium-based carbocations, easily transformed into respective ions. Such derivatives would not constitute parts of larger molecular or supramolecular systems, and the source of optical activity will originate from the single chiral substituent attached to the trityl core. This assumption excludes molecules studied previously, as they do not form carbocations or the generated tritylium did not show optical activity in the ECD. The chiral substituent may stabilize the carbocation, and this effect can be additionally supported by the presence of other electron donating groups.[20] In this study, we have focused on the chirality transfer phenomenon taking place in readily available triarylmethanol alkoxyethers **3**−**7** (Scheme 1). As

Scheme 1. Synthesis of Chiral Triarylmethanols 3−7 and Structures of Model Compounds 8

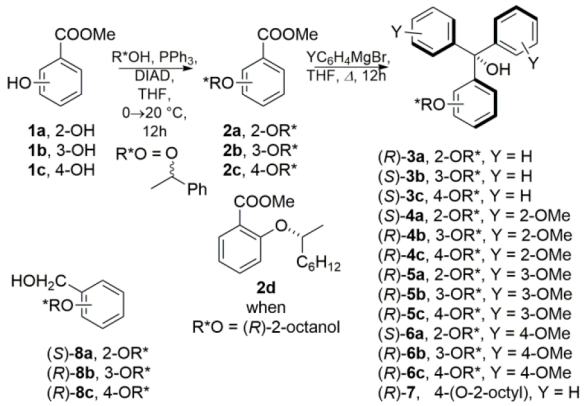

mentioned before, these compounds are characterized by the presence of a chiral substituent in one of the aryl rings, in either an *ortho*, *meta*, or *para* position to the *ipso* carbon attached to the "hub" of the propeller. This structural differentiation was supposed to show the relationship between the position of the chiral substituent (being the chirality inducer) and the efficiency of the chirality transfer process. On the other hand, methoxy substituents may play a 2-fold role—to increase steric congestion and/or to stabilize the forming carbocation—the latter may be useful at the next stage of studies.

The synthetic routes to the **3**−**7** involved Mitsunobu reaction between racemic or optically active 1-phenylethanol and commercial hydroxyesters **1a**−**1c**, followed by the additions of respective Grignard reagents to ethers **2a**−**2c**. For comparison purposes, we have synthesized triarylmethanol **7** from ether **2d** and chiral benzyl alcohols **8a**−**8c**. To study the effect of the optical purity of the sample on the possible association mode in the solid state, the selected racemic triarylmethanol *rac*-**3a** has been synthesized according to the above-mentioned procedure.

With the exception of **4a**, the ^{1}H NMR spectra of triarylmethanols, measured in $CDCl_3$, showed sharp signals, which indicated a free rotation around C−C bonds. This fact might suggest that these molecules are capable of adapting a number of easily interconverting conformations differing in the chromophore helicity, thus, of mutually canceling contributions to the CD spectra. However, despite our fears, the ECD spectra of **3**−**6** exhibited CEs in the region of trityl absorption (230−185 nm, Table 1, see the examples in Figure 1). For **3a**−**3c**, the first low energy CEs associated with ^1L_b electronic transitions appear at around 225 ± 6 nm, whereas the second intense ECD bands of ^{1}B type are found at around 200 nm. The third CEs of variable intensity appeared at a high energy region. Both the sequence and intensity of the CEs are a function of the position of a chiral substituent within skeleton (vide infra). Introduction of additional chromophoric methoxy group made very weak long-wavelength CEs (between 260 and 275 nm) visible, whereas for most of the cases **4**−**6**, the higher energy region of the spectra resemble the ECD spectra typical of chiral trityl-containing systems.

As one can deduct from the data juxtaposed in Table 1, the amplitudes of the most intense CEs, appearing at around 200 nm, ranged from rather small, $\Delta\varepsilon = -7$ ((*R*)-**6b**) to high ones, $|\Delta\varepsilon| = 80$ (for (*R*)-**3a** and (*S*)-**6a**).[21] Thus, the dynamic induction of an optical activity is a function of the substitution pattern within the given triarylmethyl system. As expected, the *ortho*-substitution with the chiral group is reflected in the most intense CEs. Having neglected the differences resulting from the opposite absolute configuration at the stereogenic centers, the direct comparison showed a significant degree of similarity between shapes of the ECD spectra of **3a**, **4a**, **5a**, **6a** (see Figure S68 showing an overlay of the traces of the corresponding ECD spectra). In these particular cases, the effect of methoxy substituents os revealed in the magnitude of the respective CEs only, and the largest steric congestion (as in the case of **4a**) was unrelated to the largest CE amplitudes. On the opposite pole, there are derivatives in which the chiral substituent occupies a *para*-position. In such cases, the effect of chiral environment on the dynamic structure of triarylmethyl chromofore, even supported by methoxy groups in *ortho* positions, could be considered rather weak. Note that the impacts of the chiral substituent in the *para* or *meta* positions on the dynamic induction of optical activity, estimated based on the CEs amplitude, were comparable.

Since some of these derivatives contain proton-donating and proton-accepting groups in the close proximity, one would expect the strong influence of the solvent polarity on the measured ECD spectra. However, the ECD spectra measured for model compounds **3a**, **3b**, and **7** in cyclohexane, acetonitrile, methanol, and acetonitrile containing up to 10% (v/v) of hexafluoro-2-propanol did not exhibit substantial

https://dx.doi.org/10.1021/acs.joc.0c02289
J. Org. Chem. 2021, 86, 643−656

Table 1. UV (ε, in dm^3·mol^{-1}·cm^{-1}) and ECD ($\Delta\varepsilon$, in dm^3·mol^{-1}·cm^{-1}) Data for 3−6 Measured in Acetonitrile and Acidified Acetonitrile Solution

	acetonitrile[a]		acidified acetonitrile[a]	
compd	$\varepsilon \times 10^4$ (nm)	$\Delta\varepsilon$ (nm)	$\varepsilon \times 10^4$ (nm)	$\Delta\varepsilon$ (nm)
3a	10.5 (190)	−9.8 (221.5), −80.0 (198), +92 (188)	n.a.	n.a.
3b	9.9 (189)	−2.7 (220.5), +16.5 (202), −6.4 (190)	n.a.	n.a.
3c	10.0 (189)	−3.2 (231.5), −8.8 (215), + 26.0 (189)	n.a.	n.a.
4a	0.6 (273), 10.2 (197), 10.3 (191)	−2.9 (282), +2.5 (268), +66.3 (200), −42.3 (190)	n.a.	n.a.
4b	0.7 (274), 9.3 (198), 10.0 (189)	−1.9 (276), −2.5 (231), −13.1 (205), +13.9 (192)	0.4 (520.5), 0.7 (404), 0.7 (271), 8.7 (201)	+2.9 (517), +2.2 (486), +1.5 (403), −2.9 (260), −1.2 (234), +1.5 (217), −8.4 (207), −6.3 (199), +2.8 (193)
4c	0.7 (273), 10.2 (199), 10.4 (190)	−0.9 (254), +8.8 (217), −18.7 (193)	2.6 (508.5), 1.4 (431), 1.1 (269), 12 (185)[b]	−1.6 (263.5), −1.3 (256), +8.9 (219), −24.3 (189)
5a	0.7 (281), 0.7 (274), 9.1 (200), 9.2 (191)	−2.0 (264), +2.2 (237), −58.1 (202.5), +71.5 (189)	n.a.	n.a.
5b	0.6 (282), 0.7 (275), 8.9 (201), 9.3 (189)	−1.2 (272.5), −1.3 (235), +1.1 (218), −12.2 (207), +7.5 (191)	n.a.	n.a.
5c	0.7 (282), 0.7 (275), 7.5 (201), 7.9 (189)	−0.9 (272), +3.3 (215), −12.0 (191.5), −12.3 (189)	0.6 (560), 0.6 (479), 0.6 (274), 8.0 (202), 12 (185)[b]	+2.4 (217), −7.7 (192), −6.9 (187)
6a	0.7 (275), 3.1 (288), 10.8 (191)	+12.5 (226.5), +82.8 (201), −74.6 (190)	4.3 (503.5), 0.8 (396.5), 1.2 (271), 12 (185)[b]	−3.6 (501.5), −1.6 (402), +2.0 (355), +3.1 (270), −6.2 (222), +26.5 (199), −11.8 (188)
6b	0.5 (283), 0.6 (276), 2.9 (227), 11 (189)	−1.1 (277), −1.3 (233), +1.8 (219), −6.7 (207), +1.8 (193)	4.9 (503), 1.5 (405.5), 1.2 (270), 12 (185)[b]	+11.3 (508), +8.0 (408), −2.8 (353), +1.6 (269), −2.0 (235), −4.0 (215), −10.6 (197), +7.5 (189)
6c	0.5 (284), 0.5 (277), 3.0 (232), 8.5 (198), 9.5 (190.5)	−0.5 (271), +4.4 (216), +4.3 (204), −15.7 (194), −17.0 (192)	8 (484), 1.8 (268), 12 (185)[b]	+1.6 (478), +1.4 (449), +6.5 (218), −13.1 (190)

[a]The concentration of analytes ranged from 1.0 to 2.0 × 10^{-4} mol L^{-1}. The spectra were recorded in pure acetonitrile or in acetonitrile containing up to 10 equiv of trifluoroacetic acid per 1 equiv of the alcohol (see the Experimental Section for details), from 600 to 185 nm, with a scan speed of 100 nm min^{-1} and with 16 accumulations. [b]The end of the measuring range.

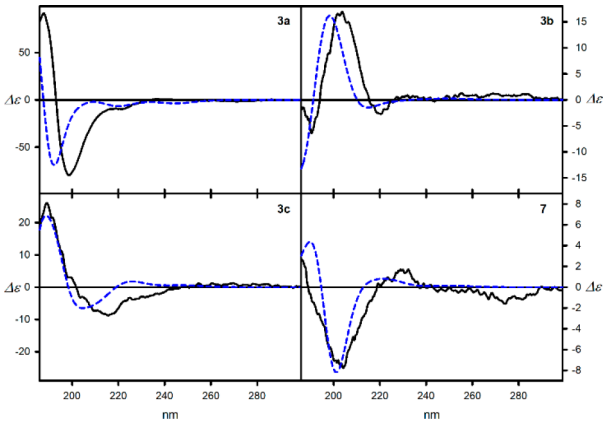

Figure 1. ECD spectra of (*R*)-**3a**, (*S*)-**3b**, (*S*)-**3c**, and (*R*)-**7** measured in acetonitrile (solid black lines) and calculated at the IEFPCM/TD-CAM-B3LYP/6-311++G(2d,2p)//IEFPCM/B3LYP/6-311++G(d,p) level (dashed blue lines). The calculated ECD spectra were Boltzmann-averaged based on $\Delta\Delta G$ values. Wavelengths were corrected to match the experimental UV maxima.

differences. Thus, we can conclude that the effect of the solvent on the observed Cotton effects can be considered as negligible for neutral species **3**−**7**.

The naturally emerging question is the one about the origin of the observed optical activity in triarylmethanols. First, we had to verify whether the 1-phenylethanoxy moiety exhibits intrinsic Cotton effects in a similar region of absorption as the trityl group. For this purpose, the model compounds **8a**−**8c** were synthesized. The ECD spectra measured for **8a**−**8c** showed the CEs of lower amplitudes and blue-shifted in relation to the ECD spectra measured for their triarylmethanol counterparts. Thus, in the triarylmethanols **3**−**6**, the intrinsic CD is overwhelmed by the CEs generated by the chiral structure of the trityl chromophore. The ultimate confirmation of the ongoing chirality transfer process was the ECD spectrum of **7**. The compound **7** does not contain any additional aromatic chromophore; thus, the observed induced optical activity originated solely from the chiral structure of the triarylmethyl moiety.

Having confirmed the dominant role of the conformation of the triarylmethyl moiety in generating a dynamic optical activity, we will give a rationale on the possible chirality transmission mechanism in compounds of this type. This can be done by two ways: either experimentally by careful analysis of X-ray data (if available) or by using theoretical calculations at a suitable level of theory. The latter approach seems to be more versatile as it allows not only for the determination of the preferred structures but also for the calculation of the ECD spectra.

The comparison and, more importantly, compliance of the experimental and theoretical ECD spectra allows, among others, for the determination of conformational equilibria, albeit not directly.[22] Since the experimental X-ray data are limited (vide infra) and the direct relationship between the structure in the solid state and structure in solution is sometimes questionable, at first we will focus on the results of the theoretical calculations. To avoid overloading the text with unnecessary details, which in turn obscure the problem, we would point out some generalities. The remaining theoretical results, less relevant to the discussion, available in the SI.

https://dx.doi.org/10.1021/acs.joc.0c02289
J. Org. Chem. 2021, 86, 643−656

The theoretical calculations, performed at the IEFPCM/B3LYP/6-311++G(d,p) level,[23,24] preceded by the systematic conformational search, allowed us to determine structures of thermally accessible conformers of compounds **3**−**7** and establish structure-forming factors. The number of conformers with relative Gibbs energy values ($\Delta\Delta G$) ranging from 0 to 2 kcal mol^{-1} vary in the number and position of the substituents. Triarylmethanols **3a**, **6a**, and **6c** are characterized by the lowest number of stable conformers, 3, 4, and 4, respectively. Introducing methoxy groups in the *meta* positions results in a significant increase of the number of thermally accessible conformers, up to 29 for **5b**. In general, the triarylmethanols having a chiral substituent on the *meta* position are characterized by the highest number of conformers in comparison to their *ortho*- and *para*-substituted counterparts (**3b**, 8; **4b**, 28; **5b**, 29; **6b**, 10 conformers). It was well-established that one of the consequences of the structural diversity, manifested, inter alia, by a large number of conformers, is the deletion of mutual contributions to the overall CD spectra by the respective conformational stereoisomers.[22] The measured chiroptical properties are linear combinations of the contribution of each species present in the sample to the total observed value. The parameter that needs to be taken into account as well is the population of a given species (conformer) in the equilibrium. Remaining in the field of ECD spectroscopy and limited the discussion to the compounds studied here, the actual contribution of individual conformational diastereoisomers to the overall spectrum is a function of the specific helicity of the chromophore, the generated rotator strengths and, last but not least, their population. Therefore, for *meta*-substituted triarylmethanols, the large number of conformers close in relative energy and characterized by opposite helicities of the chromophore resulted in deterioration of observed and calculated CEs compared to that observed in the case of compounds *ortho*-substituted by chiral moiety.

The substitution in *para* position limits the number of possible interactions between chiral fragment and remaining aryl rings in triarylmethanols **3c**, **4c**, **5c**, and **6c**. Both sides of the phenyl ring, *para*-substituted by the chiral moiety, are undistinguishable, which in turns reduces the number of possible conformers. Only in the cases of **3a** and **6c** does the population of the $\Delta\Delta G$-based lowest energy conformers exceed 50% (see Table 2). For compounds characterized by much higher number of thermally available conformers, the populations of the lowest energy one does not exceed 20%. However, it is worth noting that for the specific case, the highest abundance of a given conformer does not necessarily translate into its greatest effect on the overall ECD spectrum (vide infra).

The conformation of each conformer can be determined by a set of torsional angles α (H−O−C_{sp3}−C_{ipso}), β_1-β_3 (O−C_{sp3}−C_{ipso}−C_{ortho}), γ (C_{ipso}−O−C*−H) and ω (O−C*−C_{ipso}−C_{ortho}). The latter two torsion angles determine the conformation of the chiral substituent with regard to the aromatic ring to which it is attached. In the majority of cases, the position of proton attached to the stereogenic center, described by the γ angle, remains either (+)- or (−)-*synclinal* (*sc*). The electrostatic C_{ortho}H···O interactions between the proton from the *ortho* positions of an aromatic ring from the chiral moiety and the ether oxygen atom enforced the ω angle to adapt (+)- or (−)-*sc* conformation.

Table 2. $\Delta\Delta G$-Based Percentage Populations (Pop.) and Helicities of Trityl Chromophore Calculated for the Lowest Energy Conformers of 3a−6c at the IEFPCM/B3LYP/6-311++G(d,p) Level of Theory

compd[a]	pop.	helicity[b]
3a (conf 58)	58	*PPP*
3b (conf 28)	28	*PPP*
3c (conf 24)	28	*MMM*
4a (conf 18)	32	*PPP*
4b (conf 34)	17	*MMM*
4c (conf 1)	20	*MMM*
5a (conf 12)	32	*PPP*
5b (conf 26)	15	*MMM*
5c (conf 44)	17	*MMM*
6a (conf 13)	43	*MMM*
6b (conf 17)	20	*MMM*
6c (conf 49)	78	*MMM*

[a]The conformers are numbered according to their appearance during the conformational search. [b]Helicity was determined on the basis of the value of O−C−C_{ipso}−C_{ortho} angles (of the two possibilities the absolute values ≥90° has been chosen).

From the point of view of the possibility of exhibiting the induced optical activity, the β_1−β_3 torsion angles which determine the helicity of the trityl chromophore, either *M* ($-90° < \beta < 0°$) or *P* ($0° < \beta < 90°$) are the most important ones. This particular structural feature may be further correlated to chiroptical properties, namely the sequence of the Cotton effect appearing in the spectral region of the trityl UV absorption. Investigation of the data (Table 2, see the SI for the remaining data) led to conclusion that in the majority of cases, the trityl chromophore exhibits a tendency for adapting homohelical (quasi-symmetrical) conformation, either *MMM* or *PPP*.[25] The exceptions to adapt heterohelical conformations (*MMP* or *MPP*) are scarce. However, even when considering the lowest energy conformers only, there is no direct relationship between preferred chromophore helicity and the absolute configuration at the stereogenic center of the chiral substituent.

As far as possible, the overall helical structure of the chromophore in the isolated molecules is determined by the OH···O(R) hydrogen bond (see example structures in Figure 2a and Figures S1−S15). In turn, the OH···O(R) hydrogen bond formation controls conformation of one of the aryl rings. The (H)O···H_{ortho}C and C−H···π interactions stabilize the conformation of the second aryl ring, whereas the third one adjusts its conformation to the conformation of the remaining two that is stabilized by CH···π interactions. Thus, one would say that the structural information is transferred by the cascade process, which is, in general, similar to the recently proposed process of chirality transfer taking place in trityl-containing alcohols.[26] In the cases where OH···O(R) hydrogen bonding is not present in the molecule, the (H)O···H_{ortho}C interactions constitute the most important conformation-controlled factor. The presence or absence of an OH···O(R) hydrogen bond in a given conformer reflects in the values of the α angle. Since the general definition of the α angle is not so precise (there are three *ipso* and six *ortho* carbon atoms in the triarylmethane), we found the chiral substituent to be more important than the MeO group or the proton regardless of its position within the ring. Consistently, we have decided to prioritize the aromatic ring, substituted by the chiral moiety. Therefore, the α angle

https://dx.doi.org/10.1021/acs.joc.0c02289
J. Org. Chem. 2021, 86, 643−656

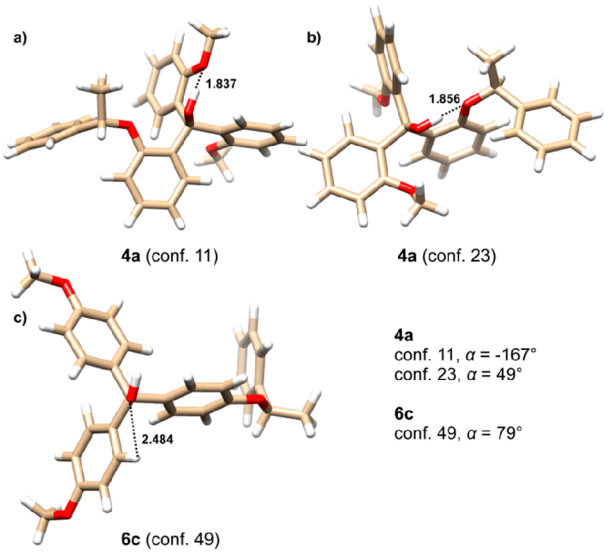

Figure 2. Examples of the low energy structures of triarylmethanols calculated at the IEFPCM/B3LYP/6-311++G(d,p) level, having conformation controlled by (a) OH···O(R*); (b) OH···OMe; and (c) sterical and (H)O···H_{ortho}C interactions. Dashed lines indicate possible attractive interactions. Distances are in angstroms. The inset shows the values of the α (H−O−C_{sp3}−C_{ipso}) angles, which determine the conformation of OH group in relation to the aromatic ring having chiral substituent.

always adopts the (+)- or (−)-*sc* conformation, with respect to the aromatic ring containing "chiral" hydrogen bond acceptor. However, in the case of competitive OH···OMe interactions with the oxygen atom from the methoxy group, the α angle is either (+)- or (−)-*antiperiplanar* (*ap*) or in the selected cases, (+)- or (−)-*sc*, depending on the spatial relation of OH group and aromatic rings with chiral and MeO substituents. Noticeably, in the particular case of **4a**, the predominance in conformational equilibrium is shown by those conformers in which the OH···OMe hydrogen bonding controls the structure.

The O−H···O distances are rather short and range from 1.834 to 1.945 Å. On the other hand, in the case of no possibility to form the intramolecular hydrogen bond, the optimal conformation of the hydroxyl group is the one that minimizes sterical interactions and at the same time allowing the (H)O···H_{ortho}C interactions. The examples of low-energy structures of triarylmethanols of conformations controlled by OH···O(R*), OH···OMe, or sterical interactions are shown in Figure 2.

A high compatibility between the experimental and theoretical ECD spectra (calculated at the IEFPCM/TD-CAM-B3LYP/6-311++G(2d,2p) level)[23,24] confirmed that both structures and relative energies of conformers have been correctly estimated. The additional value of these studies is the correlation between the signs of the Cotton effect sequence and the helicity of triarylmethyl chromophore as well as determining the particular conformer which influences the overall ECD spectrum most. As we have mentioned above, the simple relationship—the higher abundance of a given conformer, the greater effect on the overall ECD spectrum—is not always fulfilled.

For example, such counterintuitive results have been obtained for the simplest case of **3a**. As the computational analyses performed for **3a** have revealed, there are only three thermally available conformers, nos. 1, 10, and 18 (shown in Figure 3a), and each of which is stabilized by the OH···O(R) hydrogen bond along with the (H)O···H_{ortho}C and C−H···π interactions. The lowest energy conformer no. 10 of alcohol **3a** is the most abundant among all thermally accessible conformers (58% based on $\Delta\Delta G$ values). The *PPP* helicity of the chromophore corresponds to the rather unexpected negative,-positive/negative,positive/negative (∓/ ∓ /−) sequence of Cotton effects appearing in the spectral range between 230 and

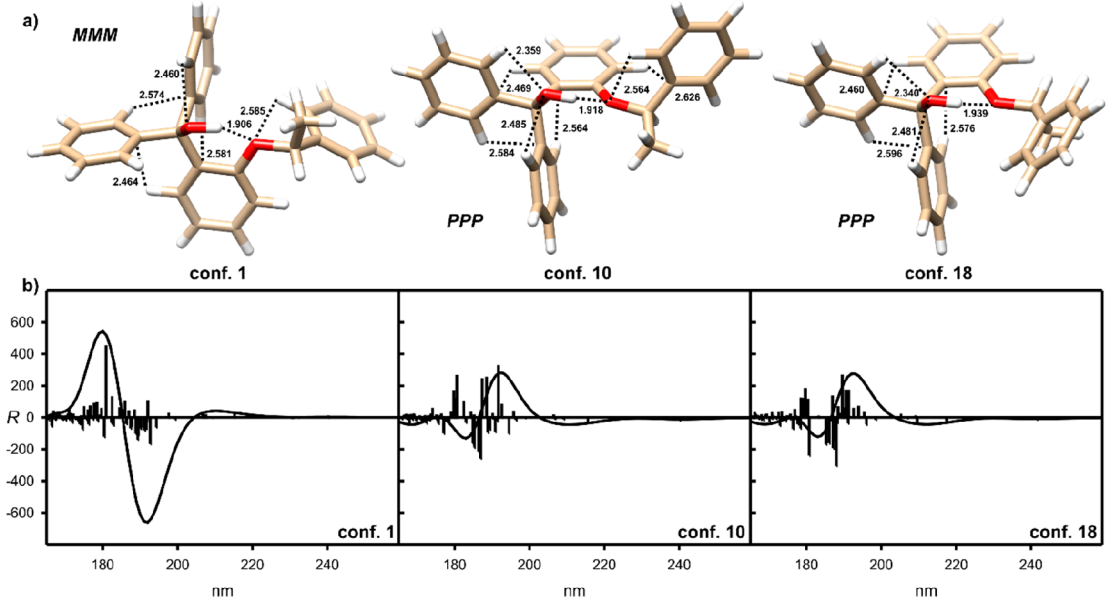

Figure 3. (a) Calculated at the IEFPCM/B3LYP/6-311++G(d,p) level low-energy conformers of **3a**, stabilized by the OH···O(R) hydrogen bond and by the (H)O···H_{ortho}C and C−H···π interactions (indicated by dashed lines). Distances are in angstroms. (b) ECD spectra calculated for individual conformers of **3a** at the IEFPCM/TD-CAM-B3LYP/6-311++G(2d,2p) level. Vertical bars represent calculated rotatory strengths. Wavelength were not corrected.

https://dx.doi.org/10.1021/acs.joc.0c02289
J. Org. Chem. 2021, 86, 643−656

180 nm (see Figure 3b). The same spectral pattern is found for the *PPP*-helical conformer no. 18, characterized by the 12% of abundance. Although both conformers 0 and 18 strongly prevail in the equilibrium (in total 70%), it is conformer no. 1 that determines the shape of the overall CD spectrum. This particular conformer is characterized by the *MMM* helicity of the chromophore, which corresponds to the ±/+ sequence of Cotton effects in the calculated ECD spectrum (see Figure 3b).

Conformer no. 1 of **3a** is characterized by the highest values of calculated Cotton effects among all thermally accessible species, which overwhelm the CEs calculated for the more abundant conformer no. 10 and for conformer no. 18. After having averaged the calculated ECD spectra accordingly to the relative populations of respective conformers, the resultant ECD spectrum has reproduced well the experimental one.

The observed induction of an optical activity provides evidence for the concept of chirality induction within triarylmethyl derivatives. However, it is more interesting to demonstrate the induced optical activity in triarylmethyl cations generated from **3**–**6** by in situ treatment of the acetonitrile solution of the respective alcohol by trifluoroacetic acid (TFA). The ECD spectra were to have shown induced CEs in the long-wavelength region, between 600 and 350 nm. Unfortunately, in the case of the most promising derivatives **3a** and **4a**, our expectations collided with reality, as we observed the complete decay of the ECD signals after acidification. Although we observed a very fast reversible color change to red, even by increasing the scanning speed to 20000 nm min^{-1},we were not able to record any ECD spectrum for an acidified sample of **3a** and **4a**. The subsequent study revealed that the carbocations generated from **3a** and **4a** rapidly underwent cleavage of the C−O ether bond, providing the respective *o*-hydroxytriphenylmethane derivatives **9a** and **9b** and acetophenone, as indicated by ^{1}H NMR (400 MHz, $CDCl_3$) measurements (see Figure 4a−c). Just after addition of anhydrous TFA to the test NMR tube, the OMe singlets, visible at around 3.5 ppm in ^{1}H NMR (400 MHz, $CDCl_3$) spectrum of **4a** (shown in Figure 4a), vanished. Instead, two sharp singlets originating from $CH_3C{=}O$ and OCH_3 protons have appeared at 2.73 and 3.72 ppm, respectively. Additionally, the aromatic region of the NMR spectrum has changed, and three sets of multiplets, of the relative integration 2:1:2, have appeared at 7.51, 7.66, and 8.05 ppm, respectively (Figure 4b). All of the signals appeared at δ 2.73, 7.51, 7.66, and 8.05 and as observed in NMR spectrum shown in Figure 4b have originated from acetophenone protons, whereas the remaining signals are ascribed to the decomposition product **9b** (the ^{1}H NMR, 400 MHz, $CDCl_3$; spectrum of isolated **9b** is shown in Figure 4c). To explain this phenomenon, we have referred to the available literature precedents. Starnes studied kinetics and mechanism of thermal or acid-promoted decomposition of, inter alia (*o*-benzyloxypheny)diphenylmethanol.[27] After treatment of the compound with TFA, the ether was cleaved and provided benzaldehyde and *o*-hydroxytriphenylmethane. Hydride transfer from the benzyl position to the positively charged carbon atom was considered a key step for the entire process. Subsequent studies by Lomas and co-workers confirmed this hypothesis.[28] Thus, on the basis of the literature evidence, we have proposed a possible decomposition mechanism of **3a** and **4a** upon acidification with TFA (Figure 4d). The reaction involves formation of the tritylium cation, and then, after [1,5]-hydride shift, a hemiacetal is

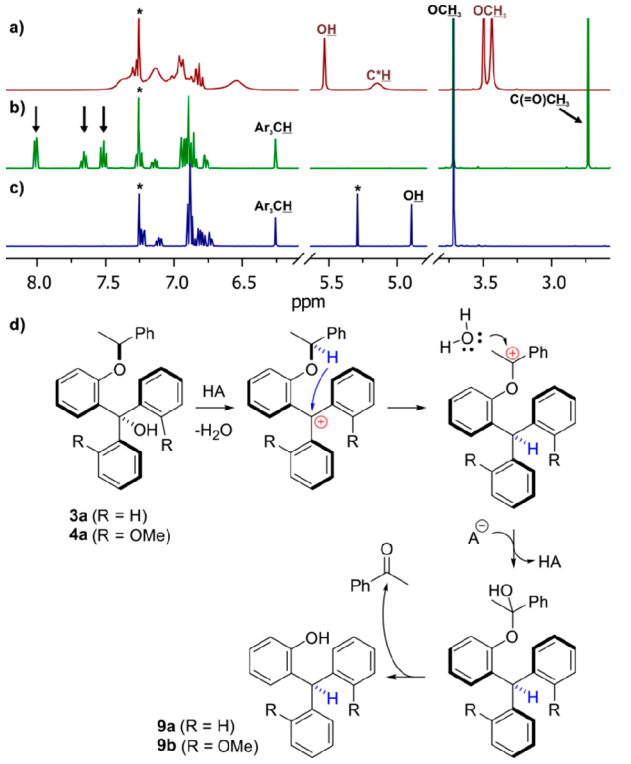

Figure 4. Traces of ^{1}H NMR (400 MHz, $CDCl_3$) spectra of (a) **4a**; (b) **4a** measured immediately upon acidification by anhydrous trifluoroacetic acid; and (c) isolated decomposition product **9b**. Arrows indicate acetophenone proton signals. Asterisks indicate trace solvent peaks. Note that the green peak appearing at 3.72 ppm (b) is obscured by the high-intensity blue peak from the lower spectrum of **9b**. Both peaks originate from OCH_3 protons. (d) Possible decomposition mechanism of *ortho*-substituted derivatives **3a** and **4a** upon acidification.

formed as a result of the nucleophilic attack of the water molecule on the positively charged benzyl carbon atom. Acidic hydrolysis of the hemiacetal led to formation of acetophenone and the respective *o*-hydroxytriphenylmethane derivatives **9a** and **9b**.

Fortunately, the other substitution patterns make the formed species more stable. The possibility for generation and the stability of the given carbocation is not directly reflected in the intensity of Cotton effects in the ECD spectra. For example, in the case of the *para*-substituted carbocation generated from **6c**, the most intense (within the compounds studied) long-wavelength UV band is observed at around 470 nm, while the ECD spectrum in this spectral region remains flat. In contrast, for all-*meta*-substituted **5b** we did not observe the generation of carbocation under these conditions. Thus, the effective induction of an optical activity is the resultant of the substituents ability to stabilize carbocation and efficiency of chirality transmission from the permanent stereogenic center to the tritylium chromophore.

The most intense chiroptical responses within the whole series were observed for carbocations generated from **6a** and **6b** (denoted here as $\mathbf{6a}^+$ and $\mathbf{6b}^+$, respectively, see Table 1). In both species, the methoxy groups are placed in *para* positions, whereas the chiral substituent occupies either the *ortho* or *meta* position. In particular, the induced CEs observed for carbocation generated from **6b** are exceptional. It should be emphasized that that acidification, except the generation of

https://dx.doi.org/10.1021/acs.joc.0c02289
J. Org. Chem. 2021, 86, 643−656

carbocation, did not lead to other changes in the constitution of the molecule of **6a** and **6b** in the time-scale of standard ^{1}H NMR measurements (see Figure 5). The appearance of signals

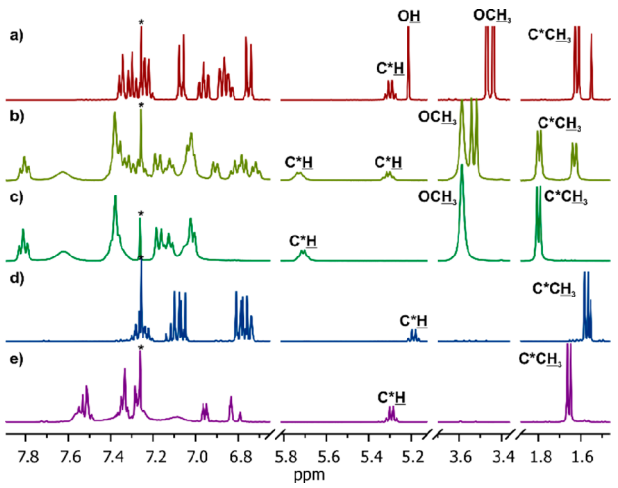

Figure 5. Traces of ^{1}H NMR (400 MHz) spectra of (a) **6a**, measured in $CDCl_3$; (b) **6a**, measured in $CDCl_3$ containing 1 equiv of anhydrous TFA; (c) **6a**, measured in $CDCl_3$ containing 2 equiv of anhydrous TFA; (d) **6b**, measured in $CDCl_3$; (e) **6b**, measured in $CDCl_3$ containing 2 equiv of anhydrous TFA. Asterisks indicate trace solvent peaks.

(at 192.8 and 194.6 ppm, for **6a**$^+$ and **6b**$^+$, respectively) characteristic for trityliums, observed in the ^{13}C{1H} NMR (101 MHz, $CDCl_3$) spectra originating from charged "central" carbon atom, has additionally confirmed formation of carbocations.[29]

We emphasize that the formation of the carbocation is fully reversible. After adding DMSO-d_6 containing some water to the NMR test tube, the measured ^{1}H NMR (400 MHz, $CDCl_3$ + TFA) spectra remain in full accordance with that measured previously for neutral **6a** and **6b**. Moreover, the ECD spectra measured for **6b**, in alternately acidified and alkalized acetonitrile solution, confirm almost perfect reversibility of the process, up to three cycles (see the SI).[30] Subsequent ECD measurements have shown that the shape of the spectrum of **6b**$^+$ did not change within 2 weeks of in situ generating the carbocation in solution.

The results of measurements in other freshly distilled and anhydrous solvents (dichloromethane, dimethylformamide, tetrahydrofuran, and DMSO) and with the use of TFA as acidifying agent, have indicated some solvent effect (see Figures S61 and S62) on ECD spectra of **6a** and **6b**. The ECD measurements performed in dichloromethane and acetonitrile have provided convergent results; generation of carbocation was observed. On the contrary, in other used solvents, we did not observe generation of carbocations **6a**$^+$ and **6b**$^+$. Although the detailed mechanism according to which the solvent may inhibit the carbocation formation is not known, it can be assumed, based on previous work,[31] that basic solvents of the THF type form oxonium compounds with triarylmethane derivatives.

To establish the counteranion effect during acid treatment, we have used acidifying agents other than TFA, namely acetic acid, methanesulfonic acid, HBF_4, and both enantiomers of camphorsulfonic acid. With the exception of acetic acid, which has turned out inefficient, the use of other acids, including the chiral ones, did not change the shape of the measured spectra of generated carbocations (see Figures S63 and S64). Therefore, even the use of both enantiomeric forms of chiral acids did not affect the chirality transfer in tritylium ions.

Unfortunately, the attempts made for isolation of **6a**$^+$ and **6b**$^+$ in analytically pure form have been unsuccessful so far. The DFT calculations (IEFPCM/TD-CAM-B3LYP/6-311++G(2d,2p)//IEFPCM/B3LYP/6-311++G(d,p) level)[23,24] allowed to shed light on the origin of the observed CEs for the most interesting example carbocation **6b**$^+$.

First, despite the large diversity of thermally accessible structures, one of the conformers found (no. 40) is dominant (the most abundant). Second, as expected, this particular conformer has also a dominant contribution to the overall UV and ECD spectra. Thus, it seems to be justified to describe the chiroptical properties of **6b**$^+$ based on this particular structure. Third, the tendency to flatten the carbocation structure does not disturb the overall propeller structure. In other words, while the central and the *ipso* carbon atoms lie in one plane, the aromatic rings, as a whole, are twisted relatively to each other. In the case of the lowest energy conformer of **6b**$^+$, which is discussed here, the twist angles ω = C_{ipso}−C$^+$−C_{ipso}−C_{ortho}, are negative and ranged from −40 to −34°. Fourth, sterical interactions between the aromatic rings of the chiral substituent and one of the phenyl ring from the triarylmethyl core induce propensity to the conformational diastereoisomerism. Fifth, the lowest energy UV absorption band, appearing at around 500 nm, is due to the HOMO−LUMO and HOMO(−1)-LUMO electronic transitions that involve orbitals from triarylmethyl core (see Figure 6). The former

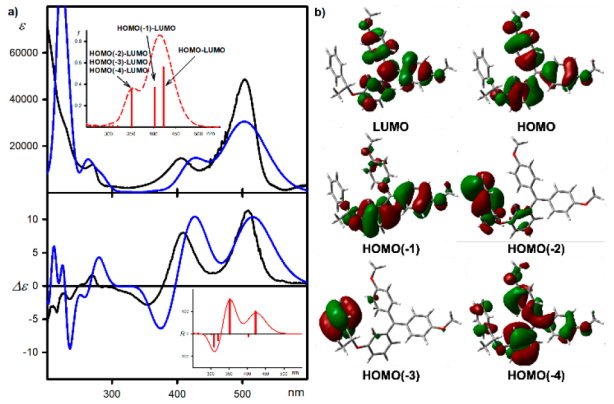

Figure 6. (a) UV (upper panel) and ECD (lower panel) spectra of **6b**$^+$ measured in the acidified acetonitrile (solid black lines) and calculated at the IEFPCM/TD-CAM-B3LYP/6-311++G(2d,2p) level (blue lines). The calculated ECD spectra were Boltzmann-averaged based on $\Delta\Delta G$ values. The wavelengths were corrected to match experimental UV maxima. Insets shows the UV and ECD spectra calculated for the lowest energy conformer of **6b**$^+$. The vertical bars represent oscillatory or rotatory strengths, respectively. (b) Molecular orbitals involved in the low energy electronic transitions in the lowest energy conformer no. 40 of **6b**$^+$.

electronic transition generates positive rotatory strength, visible in the ECD spectrum as positive low-energy CE at around 500 nm, whereas the latter electronic transition is associated with small negative rotatory strength insignificant with respect to their contribution to the overall CE. The next rotatory strength, responsible for generating the second positive CE, results from electronic transitions that mainly

https://dx.doi.org/10.1021/acs.joc.0c02289
J. Org. Chem. 2021, 86, 643−656

involve the π orbitals of the chiral substituent and the LUMO orbital. The higher energy spectral region is again dominated by the transitions that involve triarylmethyl core orbitals.

At the last stage of this study, we have referred again to the calculation results. By comparing the respective neutral and charged structures, we wanted to show the factors that determine the efficiency of the chirality transfer and thus the induction of optical activity in carbocations. The overlays of the lowest energy conformers of **6a** (conf no. 13) and **6a**$^+$ (conf no. 29), **6b** (conf no. 17) and **6b**$^+$ (conf no. 40), respectively, have shown changes, or lack thereof, in the structure upon the ionization (Figure 7).

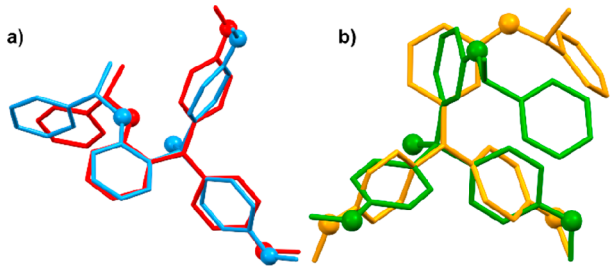

Figure 7. Overlays of the lowest energy conformers of (a) **6a** (conf no. 13, blue) and **6a**$^+$ (conf no. 29, red); (b) **6b** (conf no. 17, green) and **6b**$^+$ (conf no. 40, deep yellow), calculated at the IEFPCM/B3LYP/6-311++G(d,p) level. The oxygen atoms are shown as balls, hydrogen atoms have been omitted for clarity.

In the case of the lowest energy conformers of neutral and positively charged **6a**, ionization did not cause drastic changes in the structure. The conformation of the lowest energy conformer no. 13 of **6a** is controlled by the OH···O(R*) hydrogen bond. Upon ionization, the conformation of the lowest energy conformer no. 29 of **6a**$^+$ retained more or less the same as in its neutral counterpart. In the absence of the hydrogen bond, the structure of conformer no. 29 of **6a**$^+$ is controlled by the electrostatic interactions (R*)O···C$^+$ and by steric repulsions between the protons in *ortho* positions of phenyl rings forming tritylium ion as well as between methyl group of chiral substituent and one of the phenyl ring from the propeller. As a consequence, the chirality transfer in such neutral and charged species proceeds in a similar cascade manner as described above.

Even at first glance, the ionization of **6b** triggered significant changes in the structure of the cation. The conformation of the lowest energy conformer no. 17 of **6b** is determined by the set of the (H)O···H$_{ortho}$C and C−H···π interactions, responsible for the chirality transfer from permanent stereogenic center to the propeller. In the lowest energy conformer no. 40 of **6b**$^+$ these interactions lost their importance or were not present at all. As mentioned above, the propeller structure was flattened upon ionization; however, due to the inevitable steric repulsions between the protons in *ortho* positions, the phenyl rings are forced to be twisted relatively to each other. The sense of the propeller twist is determined by the interactions between the aromatic rings, one from the chiral substituent and one from the triarylmethyl core.

Although most of the derivatives studied here did not form crystals suitable for X-ray diffraction measurements, there are some exceptions, though. Slow evaporation of the solvents allowed to obtain crystals of (*R*)-**3a**, (*S*)-**4a**, (*R*)-**4c**, and (*S*)-**6a** (details on the crystallization of individual compounds can be found in the Supporting Information). Recently, it was found that some racemic trityl-containing compounds are prone to crystallize as solid solutions of enantiomers.[26,32] The trityl substituent can act as a supramolecular protecting group for the stereogenic center in triphenylacetyl acid derivatives, and the solid solution of enantiomers can be formed. The phenomenon of formation of solid solutions of enantiomers in organic crystals is not frequent; according to the literature data, it concerns less than 1% of racemic crystals.[33] To check the possibility to form solid solution, we have examined *rac*-**3a** as a representative example.

In accordance to the theoretical results, the predilection to the OH···O(R) hydrogen bond formation is also seen in these crystal structures. With the exception of **4c**, conformation of the molecule is additionally stabilized by intramolecular *edge-to-face* interactions between one aryl ring from the triarylmethane and the substituent's phenyl ring. The dihedral angle value between suitable aryl rings is in the range of 56.69° (for (*S*)-**6a**) and 87.51° (for (*R*)-**3a**) and the distance of the hydrogen atom from the plane designated via C atoms is in the range of 2.696 Å (for *rac*-**3a**) and 2.879 Å (for (*S*)-**4a**) (see Figure 8a). There are no strong intermolecular O−H···O

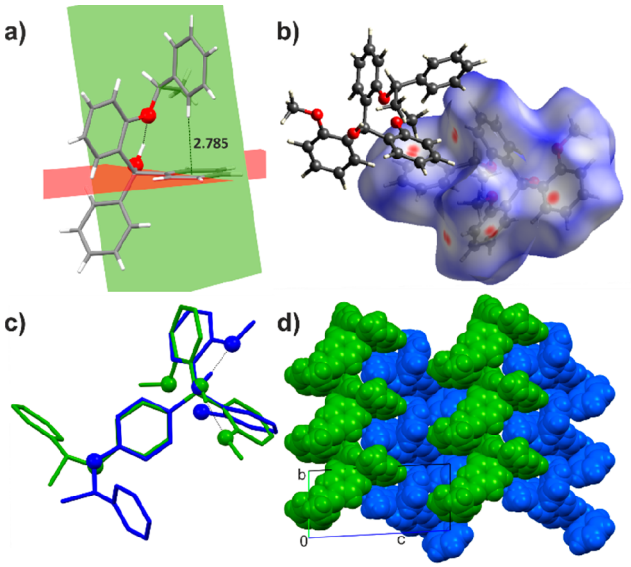

Figure 8. (a) Intramolecular *edge-to-face* interaction in molecular structure of compound **3a**; the C−H···π interactions and intramolecular O−H···O hydrogen bond are indicated as dashed lines. The distance is in angstroms. (b) C−H···π interactions found in the crystal of **4a**. (c) Overlay of X-ray diffraction determined solid-state structures of the conformational diastereoisomers (*PPP*)-**A** (green) and (*P0P*)-**B** (blue) of **4c**. (d) Folded, alternating layers of **A** and **B** molecules found in the crystal of **4c**.

hydrogen bonds in the structures of studied crystal. The van der Waals and electrostatic interactions along with directional interactions, such as weak C−H···O and C−H···π intermolecular interactions, predominate in the solid state (Figure 8b and Figure S136).

Using the *rac*-**3a** as the example, we have intended to investigate the effect of the presence of an inversion center on the intermolecular interactions in the crystal, as well as on the geometry of the molecule. From the point of view of potential applications of this and related compounds in crystal engineering, the formation of a mixed crystal would be of particular interest. However, *rac*-**3a** crystallized as racemic

https://dx.doi.org/10.1021/acs.joc.0c02289
J. Org. Chem. 2021, 86, 643−656

crystals, which means that the enantiodiscrimination in crystal structure is not disturbed. Moreover, the molecular geometry observed in crystals of (*R*)-**3a** is preserved, which confirms that the intramolecular O−H···O hydrogen bond and *edge-to-face* interaction are essential for maintaining molecular conformation.

In the exceptional case of triarylmethanol **4c**, two independent molecules denoted as **A** and **B** have been found in the asymmetric unit (Figure 8c). In the crystal, the conformational diastereoisomers (*PPP*)-**A** and (*P0P*)-**B** form separate layers, so in this particular case, one can say about a solid-state sorting phenomenon. Such sorting may be found in crystal structures, where the Z′ number is multiplied. In that case, however, we expected pseudosymmetry between the molecules to occur, which is not observed here. The surface of these layers is folded, which allows them to interpenetrate and the whole supramolecular structure is stabilized by the sets of C−H···π interactions (Figure 8d).

CONCLUSIONS

In conclusion, we have designed and proven the possibility of the dynamic induction of the optical activity in readily available latent trityl-based carbocations. These compounds are smoothly converted into corresponding cations through acidification. However, the position of the chiral substituent is crucial for the stability of the ion. The *ortho*-substituted chiral alkoxy group triarylmethanols are prone to rapid decomposition in the acidic environment.

The process of chirality transmission is demonstrated by the rise in the CEs originating mainly from the twisted form of the triarylmethyl core. The observed chirogenesis is primarily a function of the position of the chiral substituent within the triarylmethyl core. For neutral species, the *ortho*-substitution affects the structure and the ECD spectra most. As it was mentioned above, ionization may cause the cleavage of C−O(R*) bond between the chiral substituent and the phenyl ring. This is hampered by the introduction of an additional electron donating methoxy groups in *para* position of remaining aromatic rings of the chromophore.

In the cations, the combination of chiral group in *meta* and methoxy groups in *para* positions of the aryl rings forming chromophore led to the most intense chiroptical response within the whole series. The *para*- and the *meta*-substitution turned out inefficient in generation of optical activity in carbocations, within the compounds studied here.

Although the initial attempts to the use of similar compounds in asymmetric synthesis were unsuccessful,[34] we further study that is in progress in our laboratory that we believe will lead to chiral structures stable enough for efficient application as chiral Lewis acids.

EXPERIMENTAL SECTION

General Information. ^{1}H and ^{13}C{1H} NMR spectra were recorded on Bruker Ultrashield 300 MHz or Varian VNMR-S 400 MHz instruments. Chemical shifts (δ) are reported in ppm relative to $SiMe_4$ or trace solvent signals. HR-MS spectra were obtained with the use of a Bruker Impact HD, QTOF MS spectrometer. The ECD and UV spectra were measured using a JASCO J-810 spectropolarimeter at room temperature in acetonitrile and acidified acetonitrile solutions and with the use of a quartz cell of optical lengths 0.1 cm. The concentration of analytes ranged from 1.0 to 2.0 × 10^{-4} mol L^{-1}. Background spectra of the pure solvents were recorded from 600 to 185 nm with the scan speed of 100 nm min^{-1}. The ECD spectra of analytes were measured with 16 accumulations. FT-IR spectra were measured on a Nicolet iS 50 spectrometer using ATR module. A JASCO P-2000 polarimeter was used for specific optical rotation ($[\alpha]_D$) measurements (carried out at ca. 20 °C).

Column chromatography was performed on J.T. Baker silica gel 40 μm (chromatography grade). Merck Kieselgel type $60F_{254}$ analytical plates were used for TLC analyses. Melting points were measured on Büchi Melting Point B-545 and uncorrected. All reagents were used as purchased from commercial suppliers. All solvents were provided by a local supplier and were purified by conventional methods prior to use. The starting esters **1a**-**1c** are commercial and have been purchased from Sigma-Aldrich.

General Procedure for Synthesis of Chiral Hydroxy-Substituted Salicylic Esters Using *m*-Salicylic Ester As an Example. Under an argon atmosphere, ethyl 3-hydroxybenzoate (1 g, 6.02 mmol, 1 equiv), triphenylphosphine (2.15 g, 8.2 mmol, 1.36 equiv), and (*R*)-1-phenylethanol (1 g, 8.2 mmol, 1.36 equiv) were dissolved in 50 mL of freshly distilled THF. The reaction mixture was stirred for 5 min and then placed in an ice bath and cooled to 0 °C. Then DIAD (1.6 mL, 8.2 mmol, 1.36 equiv) was added dropwise over 30 min. After 15 min, the ice bath was removed and the mixture was stirred overnight at room temperature. Then THF was removed under reduced pressure, and the residue was dissolved in a mixture of diethyl ether and hexane. After a few minutes, white precipitate was formed, which was removed by filtration. The filtrate was evaporated to dryness and the crude product was purified by column chromatography on silica gel (eluent: hexane).

*Methyl (R)- or (S)-2-(1-phenylethoxy)benzoate (**2a**).* *rac*-**2a**: isolated yield, 1.5 g, 61%, colorless oil (eluent: hexane). (*R*)-**2a**: isolated yield, 0.87 g, 69%, colorless oil (eluent: hexane). (*S*)-**2a**: isolated yield, 0.92 g, 73%, colorless oil (eluent: hexane). ^{1}H NMR (300 MHz, $CDCl_3$) δ 7.75 (d, *J* = 7.6 Hz, 1H), 7.67−7.16 (m, 6H), 7.16−6.66 (m, 2H), 5.38 (q, *J* = 12.7, 6.3 Hz, 1H), 3.91 (s, 3H), 1.67 (d, *J* = 6.4 Hz, 3H). ^{13}C{1H} NMR (101 MHz, $CDCl_3$) δ 167.0, 157.2, 142.8, 132.9, 131.4, 128.6, 127.5, 125.6, 121.2, 120.18, 115.3, 51.9, 24.3. ATR-IR 3062, 3029, 2979, 2949, 1726, 1599, 1486, 1448, 1432, 1300, 1240, 1080, 751, 699 cm^{-1}. ESI HRMS *m*/*z* calcd for $C_{16}H_{16}O_3Na$ $[M + Na]^+$: 279.0992, found 279.0988. (*R*)-**2a**: $[\alpha]_D$ = −28.9 (*c* 1.44, MeCN). (*S*)-**2a**: $[\alpha]_D$ = +37.8 (*c* 0.48, MeCN).

*Ethyl (R)- or (S)-3-(1-Phenylethoxy)benzoate (**2b**).* (*S*)-**2b**: isolated yield, 1.4 g, 78%, colorless oil (eluent: hexane). (*R*)-**2b**: isolated yield, 2.6 g, 82%, colorless oil (eluent: hexane). ^{1}H NMR (400 MHz, $CDCl_3$) δ 7.62−7.48 (m, 2H), 7.41−7.19 (m, 6H), 7.07−6.96 (m, 1H), 5.36 (q, *J* = 6.4 Hz, 1H), 4.32 (q, *J* = 7.1 Hz, 2H), 1.65 (d, *J* = 6.4 Hz, 3H), 1.36 (t, *J* = 7.1 Hz, 3H). ^{13}C{1H} NMR (101 MHz, $CDCl_3$) δ 166.4, 157.8, 142.6, 131.6, 129.2, 128.6, 127.5, 125.6, 121.8, 120.5, 116.7, 76.1, 60.9, 24.3, 14.3. ATR-IR 3063, 3031, 2979, 2931, 2903, 1714, 1582, 1486, 1442, 1271, 1213, 1098, 1068, 1025, 956, 752, 682 cm^{-1}. ESI HRMS *m*/*z* calcd for $C_{17}H_{18}NaO_3$ $[M + H]^+$: 293.1148, found 293.1139. (*R*)-**2b**: $[\alpha]_D$ = +5.1 (*c* 1.1, MeCN). (*S*)-**2b**: $[\alpha]_D$ = −4.7 (*c* 1.23, MeCN).

*Ethyl (R) or (S)-4-(1-Phenylethoxy)benzoate (**2c**).* (*R*)-**2c**: isolated yield, 1.8 g, 56%, colorless oil (eluent: hexane). (*S*)-**2c**, isolated yield, 1.5 g, 84%, colorless oil (eluent: hexane). ^{1}H NMR (300 MHz, $CDCl_3$) δ 7.90 (d, *J* = 8.9 Hz, 2H), 7.44−7.14 (m, 5H), 6.86 (d, *J* = 8.9 Hz, 2H), 5.38 (q, *J* = 6.4 Hz, 1H), 4.30 (q, *J* = 7.1 Hz, 2H), 1.66 (d, *J* = 6.4 Hz, 3H), 1.34 (t, *J* = 7.1 Hz, 3H). ^{13}C{1H} NMR (101 MHz, CDCl3) δ 166.3, 161.6, 142.4, 131.3, 128.7, 127.6, 125.4, 122.7, 115.3, 76.1, 60.5, 24.4, 14.3. ATR-IR 3062, 3029, 2979, 2930, 2903, 1707, 1604, 1580, 1507, 1450, 1366, 1272, 1243, 1165, 1100, 1066, 1010, 930, 846, 768, 696 cm^{-1}. ESI HRMS *m*/*z* calcd for $C_{17}H_{18}NaO_3$ $[M + Na]^+$: 293.1148, found 293.1143. (*R*)-**2c**: $[\alpha]_D$ = +3.9 (*c* = 1.15, MeCN). (*S*)-**2c**: $[\alpha]_D$ = −5.1 (*c* = 1.08, MeCN).

*(R)-1-Bromo-2-(octan-2-yloxy)benzene (**2d**).* Isolated yield, 0.78 g, 72%, colorless oil (eluent: hexane). ^{1}H NMR (300 MHz, DMSO) δ 7.60−7.46 (m, 1H), 7.31 (ddd, *J* = 8.9, 7.4, 1.6 Hz, 1H), 7.11 (dd, *J* = 8.3, 1.2 Hz, 1H), 6.85 (td, *J* = 7.8, 1.4 Hz, 1H), 4.64−4.33 (m, 1H), 1.85−1.04 (m, 13H), 0.84 (t, *J* = 6.7 Hz, 3H). ^{13}C{1H} NMR (101 MHz, $CDCl_3$) δ 154.8, 133.4, 128.2, 121.6, 115.2, 113.5, 75.8, 36.4, 31.8, 29.2, 25.4, 22.6, 19.7, 14.1. ATR-IR 3063, 2952, 2927, 2856, 1585, 1572, 1474, 1442, 1377, 1273, 1244, 1162, 1127, 1047, 1029,

https://dx.doi.org/10.1021/acs.joc.0c02289
J. Org. Chem. 2021, 86, 643−656

974, 937, 743,664 cm^{-1}. ESI HRMS *m/z* calcd for $C_{17}H_{18}NaO_3$ $[M + Na]^+$: 307.0668, found 307.0665. $[\alpha]_D = -16.7$ (*c* 1.02, MeCN).

General Procedure for Synthesis of Triarylmethanol Derivatives Using 6a as an Example. Under an argon atmosphere, magnesium turnings (0.135 g, 5.56 mmol, 2.85 equiv) were added to a 50 mL two-neck round-bottomed flask, equipped with a reflux condenser and containing 25 mL of a freshly distilled THF. To the mixture 4-bromoanisole (1.04 g, 5.56 mmol, 2.85 equiv) was added dropwise via syringe in a few portions. After the first addition of 4-bromoanisole, the reaction mixture was placed in an ultrasonic bath and sonicated until the reaction was started. Then the ultrasonic bath was replaced with a heating mantle and a magnetic stirrer. The remaining amount of aryl bromide was added for over 15 min and refluxed until all the magnesium dissolved. The reaction was cooled to the room temperature, and (*S*)-2-(1-phenylethoxy)benzoate (**2a**, 0.5 g, 1.95 mmol, 1 equiv) was added dropwise to a vigorously stirred solution. After 30 min, the reaction was heated up and refluxed overnight. After cooling to the room temperature, a saturated solution of ammonium chloride was added to the reaction mixture and the whole suspension was stirred for 15 min. The organic layer was separated, and an aqueous phase was extracted with diethyl ether (3 × 10 mL). The combined organic layers were washed with brine and dried over anhydrous Na_2SO_4. The drying agent was removed by filtration, the filtrate was evaporated to dryness, and the crude product was purified by a column chromatography on silica gel (eluent: hexane/AcOEt, 9:1). Resulting white solid was crystallized from the mixture of toluene and hexane.

*rac- or (R)-Diphenyl(2-(1-phenylethoxy)phenyl)methanol (**3a**).* *rac*-**3a**: isolated yield, 0.37 g, 61% (eluent: hexane/AcOEt, 9:1), colorless crystals. (*R*)-**3a**: isolated yield, 0.73 g, 49% (eluent: hexane/AcOEt, 9:1), colorless crystals. ^1H NMR (300 MHz, $CDCl_3$) δ 7.44−6.98 (m, 14H), 6.95−6.83 (m, *J* = 6.7, 2.8 Hz, 2H), 6.82−6.64 (m, *J* = 11.1, 6.1, 2.3 Hz, 2H), 6.52 (dd, *J* = 7.6, 1.7 Hz, 1H), 5.49 (s, 1H), 5.21 (q, *J* = 6.4 Hz, 1H), 1.25 (d, *J* = 6.4 Hz, 3H). $^{13}C\{1H\}$ NMR (101 MHz, $CDCl_3$) δ 155.3, 146.6, 146.3, 142.1, 135.6, 130.0, 128.6, 128.6, 127.8, 127.8, 127.7, 127.6, 127.0, 126.9, 125.2, 120.0, 113.5, 82.0, 76.6, 23.9. ATR-IR 3508, 3087, 3063, 3026, 2980, 2885, 1597, 1580, 1477, 1447, 1359, 1349, 1284, 1228, 1163, 1120, 1065, 1017, 1007, 996, 930, 887, 760, 746, 695 cm^{-1}. ESI HRMS *m/z* calcd for $C_{27}H_{24}O_2Na$ $[M + Na]^+$: 403.1669, found 403.1658. (*R*)-**3a**: $[\alpha]_D = -51.4$ (*c* 1.45, MeCN). *rac*-**3a**: Mp 127−128 °C. (*R*)-**3a**; Mp 110−112 °C.

*(S)-Diphenyl(3-(1-phenylethoxy)phenyl)methanol (**3b**).* Isolated yield, 0.70 g, 35%, colorless oil, eluent: hexane/AcOEt, 9:1. ^1H NMR (300 MHz, $CDCl_3$) δ 7.33−7.06 (m, 17H), 6.89−6.65 (m, 3H), 5.18 (q, *J* = 6.4 Hz, 1H), 2.71 (s, 1H), 1.57 (d, *J* = 6.4 Hz, 3H). $^{13}C\{1H\}$ NMR (101 MHz, $CDCl_3$) δ 157.4, 148.2, 146.7, 146.5, 142.9, 128.8, 128.5, 127.8, 127.8, 127.7, 127.3, 127.1, 127.1, 125.6, 120.2, 116.0, 114.8, 81.8, 75.8, 24.3. ATR-IR 3557, 3466, 3058, 3026, 2976, 2927, 1595, 1578, 1484, 1445, 1372, 1312, 1285, 1242, 1144, 1068, 1011, 969, 928, 903, 753, 695 cm^{-1}. ESI HRMS *m/z* calcd for $C_{27}H_{24}O_2Na$ $[M + Na]^+$: 403.1669, found 403.1666. $[\alpha]_D = +13.3$ (*c* 1.05, MeCN).

*(S)-Diphenyl(4-(1-phenylethoxy)phenyl)methanol (**3c**).* Isolated yield, 0.17 g, 9%, colorless oil, eluent: hexane/AcOEt, 9:1. ^1H NMR (400 MHz, $CDCl_3$) δ 7.48−6.63 (m, 19H), 5.28 (q, *J* = 6.5 Hz, 1H), 2.70 (s, 1H), 1.67−1.50 (d, 3H). $^{13}C\{1H\}$ NMR (101 MHz, $CDCl_3$) δ 157.1, 147.0, 143.1, 139.0, 129.1, 128.6, 127.8, 127.4, 127.0, 125.4, 115.0, 81.6, 75.9, 24.5. ATR-IR 3551, 3461, 3059, 3029, 2977, 2929, 2890, 1605, 1583, 1505, 1446, 1372, 1291, 1240, 1176, 1155, 1067, 1030, 1008, 930, 894, 828, 756, 696, 627 cm^{-1}. ESI HRMS *m/z* calcd for $C_{27}H_{24}O_2Na$ $[M + Na]^+$: 403.1669, found 403.1668. $[\alpha]_D = +10.5$ (*c* 0.5, MeCN).

*(S)-Bis(2-methoxyphenyl)(2-(1-phenylethoxy)phenyl)methanol (**4a**).* Isolated yield, 0.14 g, 16% (eluent: hexane/AcOEt, 9:1), colorless crystals. ^1H NMR (300 MHz, $CDCl_3$) δ 7.48−6.41 (m, 17H), 5.53 (s, 1H), 5.15 (s, 1H), 3.47 (d, *J* = 17.3 Hz, 6H), 1.26 (s, 3H). $^{13}C\{1H\}$ NMR (101 MHz, $CDCl_3$) δ 157.7, 143.1, 133.2, 130.7, 129.9, 129.7, 128.3, 127.6, 127,1, 125.3, 120.4, 119.9, 119.3, 119.3, 112.6, 80.3, 75.3, 55.8, 55.6, 24.5. ATR-IR 3494, 3060, 3026, 2926, 2853, 1596, 1582, 1485, 1449, 1434, 1372, 1284, 1233, 1025, 908, 748 699 cm^{-1}. ESI HRMS *m/z* calcd for $C_{29}H_{28}O_4Na$ $[M + Na]^+$: 463.1880, found 463.1893. $[\alpha]_D = +52.4$ (*c* 0.55, MeCN). Mp 144−146 °C.

*(R)-Bis(2-methoxyphenyl)(3-(1-phenylethoxy)phenyl)methanol (**4b**).* Isolated yield, 0.19 g, 22%, colorless oil, slowly solidifying after a few weeks, eluent: hexane/AcOEt, 9:1. ^1H NMR (300 MHz, $CDCl_3$) δ 7.37−7.13 (m, *J* = 8.3, 4.7 Hz, 7H), 7.08 (t, *J* = 7.9 Hz, 1H), 6.94−6.62 (m, 9H), 5.35−5.04 (m, *J* = 13.6, 7.2 Hz, 2H), 3.44 (d, *J* = 6.2 Hz, 6H), 1.56 (d, *J* = 6.4 Hz, 3H). $^{13}C\{1H\}$ NMR (75 MHz, $CDCl_3$) δ 157.5, 157.4, 157.1, 148.1, 143.3, 134.2, 133.9, 129.6, 128.6, 128.4, 125.8, 120.3, 114.7, 112.4, 81.2, 75.6, 55.5, 24.3. ATR-IR 3511, 3061, 2976, 2931, 2835, 1736, 1597, 1581, 1484, 1455, 1434, 1371, 1284, 1231, 1024, 915, 751, 699, 638 cm^{-1}. ESI HRMS *m/z* calcd for $C_{29}H_{28}O_4Na$ $[M + Na]^+$: 463.1880, found 463.1871. $[\alpha]_D = +5.4$ (*c* 0.53, MeCN). Mp 55−55.5 °C.

*(R)-Bis(2-methoxyphenyl)(4-(1-phenylethoxy)phenyl)methanol (**4c**).* Isolated yield, 0.12 g, 12% (eluent: hexane/AcOEt, 9:1), white crystals. ^1H NMR (300 MHz, $CDCl_3$) δ 7.33−7.08 (m, 7H), 7.00 (d, *J* = 8.7 Hz, 2H), 6.89 (td, *J* = 7.5, 1.6 Hz, 2H), 6.78 (dd, *J* = 13.8, 7.8 Hz, 4H), 6.68 (d, *J* = 8.8 Hz, 2H), 5.23 (q, *J* = 6.4 Hz, 1H), 5.15 (s, 1H), 3.39 (d, *J* = 9.2 Hz, 6H), 1.55 (d, *J* = 6.4 Hz, 3H). $^{13}C\{1H\}$ NMR (75 MHz, $CDCl_3$) δ 157.4, 156.6, 143.4, 138.5, 134.6, 129.4, 128.9, 128.5, 125.6, 120.3, 114.8, 112.4, 80.8, 75.9, 55.6, 24.5. ATR-IR 3490, 3059, 2987, 2967, 2933, 2835, 1597, 1582, 1505, 1484, 1448, 1434, 1370, 1282, 1239, 1175, 1019, 1006, 916, 763, 750, 703, 625, 516 cm^{-1}. ESI HRMS *m/z* calcd for $C_{29}H_{28}O_4Na$ $[M + Na]^+$: 463.1880, found 463.1882. $[\alpha]_D = -21.9$ (*c* 0.5, MeCN). Mp 117−118 °C.

*(R)-Bis(3-methoxyphenyl)(2-(1-phenylethoxy)phenyl)methanol (**5a**).* Isolated yield, 0.49 g, 28% (eluent: hexane/AcOEt, 9:1), colorless crystals. ^1H NMR (300 MHz, $CDCl_3$) δ 7.31−6.37 (m, 17H), 5.49 (s, 1H), 5.22 (q, *J* = 6.4 Hz, 1H), 3.76 (d, *J* = 5.9 Hz, 6H), 1.28 (d, *J* = 6.4 Hz, 3H). $^{13}C\{1H\}$ NMR (75 MHz, $CDCl_3$) δ 159.3, 155.3, 148.1, 147,9, 142.1, 135.4, 130.1, 128.6, 125.3, 120.6, 120.2, 113.5, 112.7, 82.0, 55.2, 23.9. ATR-IR 3506, 3060, 3025, 2924, 2852, 1595, 1581, 1484, 1448, 1434, 1371, 1284, 1235, 1026, 1010, 933, 909, 748, 730, 698 cm^{-1}. ESI HRMS *m/z* calcd for $C_{29}H_{28}O_4Na$ $[M + Na]^+$: 463.1880, found 463.1873. $[\alpha]_D = -29.3$ (*c* 0.63, MeCN). Mp 145−147 °C.

*(R)-Bis(3-methoxyphenyl)(3-(1-phenylethoxy)phenyl)methanol (**5b**).* Isolated yield, 0.42 g, 40%, yellow oil, eluent: hexane/AcOEt, 9:1. ^1H NMR (300 MHz, $CDCl_3$) δ 7.41−7.05 (m, 9H), 6.85−6.65 (m, 8H), 5.18 (q, *J* = 6.4 Hz, 1H), 3.72 (d, *J* = 4.6 Hz, 6H), 2.72 (s, 1H), 1.57 (d, *J* = 6.4 Hz, 3H). $^{13}C\{1H\}$ NMR (75 MHz, $CDCl_3$) δ 159.2, 157.5, 148.2, 148.1, 142.9, 128.8, 128.5, 125.6, 120.4, 120.2, 114.9, 112.5, 81.8, 55.2, 24.3. ATR-IR 3342, 3061, 2977, 2835, 1596, 1485, 1449, 1434, 1372, 1287, 1239, 11147, 1041, 881, 769, 699 cm^{-1}. ESI HRMS *m/z* calcd for $C_{29}H_{28}O_4Na$ $[M + Na]^+$: 463.1880, found 463.1874. $[\alpha]_D = +1.3$ (*c* 0.54, MeCN).

*(R)-Bis(3-methoxyphenyl)(4-(1-phenylethoxy)phenyl)methanol (**5c**).* Isolated yield, 0.18 g, 17%, colorless oil, eluent: hexane/AcOEt, 9:1. ^1H NMR (300 MHz, $CDCl_3$) δ 7.33 (m, 4H), 7.20 (m, 3H), 7.06 (d, *J* = 8.8 Hz, 2H), 6.90−6.68 (m, 8H), 5.27 (q, *J* = 6.4 Hz, 1H), 3.71 (s, 6H), 2.70 (s, 1H), 1.62 (d, *J* = 6.4 Hz, 3H). $^{13}C\{1H\}$ NMR (101 MHz, $CDCl_3$) δ 159.1, 157.2, 148.5, 143.1, 138.8, 129.0, 128.7, 128.6, 127.4, 125.5, 120.4, 115.1, 113.7, 112.3, 75.9, 55.1, 29.7, 24.5. ATR-IR 3396, 2973, 2834, 1596, 1504, 1487, 1450, 1450, 1433, 1372, 1313, 1286, 1240, 1171, 1146, 1039, 945, 930, 833, 773, 761, 699 cm^{-1}. ESI HRMS *m/z* calcd for $C_{29}H_{28}O_4Na$ $[M + Na]^+$: 463.1880, found 463.1872. $[\alpha]_D = +1.6$ (*c* 0.48, MeCN).

*(S)-Bis(4-methoxyphenyl)(2-(1-phenylethoxy)phenyl)methanol (**6a**).* Isolated yield, 0.23 g, 27% (eluent: hexane/AcOEt, 9:1), colorless crystals. ^1H NMR (300 MHz, $CDCl_3$) δ 7.25−7.15 (m, 7H), 7.08 (dt, *J* = 7.9, 1.7 Hz, 1H), 6.92 (dd, *J* = 6.6, 2.9 Hz, 2H), 6.89−6.79 (m, 4H), 6.77−6.65 (m, 2H), 6.54 (dd, *J* = 7.6, 1.6 Hz, 1H), 5.45 (s, 1H), 5.22 (q, *J* = 6.4 Hz, 1H), 3.82 (d, *J* = 6.4 Hz, 6H), 1.30 (d, *J* = 6.4 Hz, 3H). $^{13}C\{1H\}$ NMR (75 MHz, $CDCl_3$) δ 158.5, 155.4, 142.2, 139.3, 139.0, 136.0, 130.1, 129.0, 128.6, 125.3, 120.1, 113.5, 113.0, 81.6, 55.3, 24.1. ATR-IR 3534, 2997, 2953, 2930, 2894, 2833, 1655, 1597, 1580, 1505, 1480, 1448, 1296, 1242, 1227, 1176, 1105, 1067,

https://dx.doi.org/10.1021/acs.joc.0c02289
J. Org. Chem. 2021, 86, 643−656

1031, 935, 831, 813, 755, 704, 606 cm^{-1}. ESI HRMS m/z calcd for $C_{29}H_{28}O_4Na$ $[M + Na]^+$: 463.1880, found 463.1888. $[\alpha]_D$ = +59.5 (c 0.43, MeCN). Mp 171−172 °C.

*(R)-Bis(4-methoxyphenyl)(3-(1-phenylethoxy)phenyl)methanol (**6b**).* Isolated yield, 0.31 g, 36%, colorless oil, eluent: hexane/AcOEt, 9:1. ^1H NMR (300 MHz, $CDCl_3$) δ 7.39−7.18 (m, 6H), 7.16−6.96 (m, 5H), 6.89−6.67 (m, 7H), 5.19 (q, J = 6.4 Hz, 1H), 3.80 (d, J = 1.9 Hz, 6H), 2.63 (s, 1H), 1.57 (d, J = 6.5 Hz, 3H). $^{13}C\{1H\}$ NMR (75 MHz, $CDCl_3$) δ 158.5, 158.5, 157.4, 148.7, 143.0, 139.4, 139.2, 129.0, 128.5, 125.7, 120.1, 116.0, 113.1, 81.3, 75.9, 55.2, 24.3. ATR-IR 3481, 2929, 2834, 1605, 1580, 1507, 1481, 1439, 1293, 1243, 1173, 1068, 1029, 830, 813, 790, 760, 698 cm^{-1}. ESI HRMS m/z calcd for $C_{29}H_{28}O_4Na$ $[M + Na]^+$: 463.1880, found 463.1972. $[\alpha]_D$ = +1.6 (c 1.12, MeCN).

*(R)-Bis(4-methoxyphenyl)(4-(1-phenylethoxy)phenyl)methanol (**6c**).* Isolated yield, 0.32 g, 31%, colorless oil, eluent: hexane/AcOEt, 9:1. ^1H NMR (300 MHz, $CDCl_3$) δ 7.40−7.19 (m, 5H), 7.18−6.99 (m, 6H), 6.78 (dd, J = 8.6, 7.1 Hz, 6H), 5.27 (q, J = 6.4 Hz, 1H), 3.78 (s, 6H), 2.62 (s, 1H), 1.61 (d, J = 6.4 Hz, 3H). $^{13}C\{1H\}$ NMR (75 MHz, $CDCl_3$) δ 158.5, 157.1, 143.2, 139.7, 139.6, 129.0, 128.6, 125.5, 115.0, 113.1, 81.1, 76.0, 55.2, 24.5. ATR-IR 3481, 3032, 2976, 2930, 2903, 2835, 1605, 1581, 1504, 1452, 1372, 1295, 1239, 1173, 1030, 825, 760, 699, 607, 583 cm^{-1}. ESI HRMS m/z calcd for $C_{29}H_{28}O_4Na$ $[M + Na]^+$: 463.1880, found 463.1876. $[\alpha]_D$ = −18.2 (c 0.38, MeCN).

*(R)-(3-(Octan-2-yloxy)phenyl)diphenylmethanol (**7**).* Under an argon atmosphere, (*R*)-1-bromo-2-(octan-2-yloxy)benzene (**2d**, 0.33 g, 1.16 mmol, 1 equiv) was dissolved in 10 mL of a freshly distilled THF. The reaction was cooled to −78 °C, and *n*-BuLi (0.46 mL, 1.16 mmol, 1 equic, 2.5 M solution in hexanes) was slowly added dropwise to the mixture. The mixture was being stirred for 0.5 h in dry ice/acetone bath. Benzophenone (0.219 g, 1.16 mmol, 1 equiv) dissolved in 10 mL of dry THF was added dropwise over 15 min. The cooling bath was then removed, and the reaction was left stirring overnight. The saturated solution of ammonium chloride (20 mL) was added and the mixture was extracted with diethyl ether (3 × 10 mL). The combined organic phases were washed with brine (20 mL) and dried over anhydrous sodium sulfate. The drying agent was removed by filtration. The solvent was evaporated under reduced pressure, and the crude product was purified using a column chromatography on silica gel (eluent: hexane/AcOEt, 9:1) resulting in the desired product.

Isolated yield, 0.14 g, 32%, colorless oil. ^1H NMR (300 MHz, DMSO-d_6) δ 7.58−6.60 (m, 14H), 5.63 (s, 1H), 4.48−4.23 (m, 1H), 1.15 (m, 8H), 0.87 (m, 8H). $^{13}C\{1H\}$ NMR (101 MHz, $CDCl_3$) δ 155.3, 146.6, 146.5, 135.9, 130.3, 128.6, 127.8, 127.7, 127.6, 127.5, 126.9, 126.8, 119.6, 112.6, 82.0, 73.6, 36.1, 31.6, 29.2, 24.9, 22.6, 18.9, 14.1. ATR-IR 3508, 3058, 3026, 2953, 2926, 2855, 1597, 1582, 1481, 1446, 1377, 1284, 1225, 1119, 1018, 750, 698 cm^{-1}. ESI HRMS m/z calcd for $C_{27}H_{32}O_2Na$ $[M + Na]^+$: 411.2295, found 411.2311. $[\alpha]_D$ = −19.4 (c 1.19, MeCN).

General Procedure for Reduction of Salicylic Esters. Under an argon atmosphere, lithium aluminum hydride (0.15 g, 4 mmol, 3 equiv) was slowly added to freshly distilled THF (10 mL) at 0 °C. The respective salicylic ester **2** (0.36 g, 1.3 mmol, 1 equiv) dissolved in THF (10 mL) was added dropwise to the suspension. The progress of the reaction was monitored by TLC. When the conversion of substrate was completed, water (20 mL) was added slowly at 0 °C, and the reaction mixture was extracted with diethyl ether (3 × 10 mL). The combined organic layers were washed with brine, dried over anhydrous sodium sulfate and evaporated under reduced pressure after removing the drying agent by filtration. The crude product was purified by flash chromatography on silica gel (eluent: dichloromethane).

*(S)-(2-(1-Phenylethoxy)phenyl)methanol (**8a**).* Isolated yield, 0.2 g, 88%, colorless oil, eluent: dichloromethane. ^1H NMR (300 MHz, $CDCl_3$) δ 7.44−7.19 (m, 6H), 7.11 (dt, J = 8.0, 1.7 Hz, 1H), 6.88 (t, J = 7.4 Hz, 1H), 6.73 (d, J = 8.2 Hz, 1H), 5.38 (q, J = 6.4 Hz, 1H), 4.77 (q, 2H), 2.42 (s, 1H), 1.67 (d, J = 6.4 Hz, 3H). $^{13}C\{1H\}$ NMR (101 MHz, $CDCl_3$) δ 155.7, 142.6, 129.5, 128.7, 127.6, 125.3, 120.6, 113.0, 76.1, 62.4, 24.4. ATR-IR 3347, 3062, 3030, 2976, 2927, 2868, 1601, 1588, 1487, 1451, 1371, 1284, 1232, 1112, 1067, 1028, 1009, 997, 933, 748, 697 cm^{-1}. ESI HRMS m/z calcd for $C_{15}H_{16}O_2Na$ $[M + Na]^+$: 251.1043, found 251.1044. $[\alpha]_D$ = +4.3 (c 0.64, MeCN).

*(R)-(3-(1-Phenylethoxy)phenyl)methanol (**8b**).* Isolated yield, 0.18 g, 79%, colorless oil, eluent: dichloromethane. ^1H NMR (300 MHz, $CDCl_3$) δ 7.46−7.07 (m, 6H), 7.00−6.81 (m, 2H), 6.77 (dd, J = 8.2, 2.3 Hz, 1H), 5.33 (q, J = 6.4 Hz, 1H), 4.59 (s, 2H), 1.63 (m, 4H). $^{13}C\{1H\}$ NMR (101 MHz, $CDCl_3$) δ 158.1, 143.1, 142.3, 129.4, 128.6, 127.4, 125.5, 119.1, 114.9, 114.4, 75.8, 65.1, 24.4. ATR-IR 3321, 3061, 3030, 2977, 2927, 2867, 1583, 1486, 1446, 1372, 1256, 1151, 1067, 1011, 998, 952, 879, 760, 747, 696 cm^{-1}. ESI HRMS m/z calcd for $C_{15}H_{16}O_2Na$ $[M + Na]^+$: 251.1043, found 251.1040. $[\alpha]_D$ = +15.1 (c 0.47, MeCN).

*(R)-(4-(1-Phenylethoxy)phenyl)methanol (**8c**).* Isolated yield, 0.17 g, 75%, colorless oil, eluent: dichloromethane. ^1H NMR (300 MHz, $CDCl_3$) δ 7.47−7.02 (m, 7H), 6.84 (d, J = 8.6 Hz, 2H), 5.30 (q, J = 6.4 Hz, 1H), 4.55 (s, 2H), 1.63 (d, J = 6.4 Hz, 3H), 1.54 (s, 1H). $^{13}C\{1H\}$ NMR (101 MHz, $CDCl_3$) δ 157.5, 143.0, 133.0, 128.6, 128.5, 127.4, 125.5, 115.9, 75.9, 65.0, 24.4. ATR-IR 3319, 3061, 3030, 2977, 2927, 2869, 1610, 1585, 1508, 1449, 1372, 1298, 1234, 1172, 1068, 1027, 1008, 997, 930, 819, 759, 698 cm^{-1}. ESI HRMS m/z calcd for $C_{15}H_{16}O_2Na$ $[M + Na]^+$: 251.1043, found 251.1040. $[\alpha]_D$ = −16.1 (c 0.47, MeCN).

General Procedure for the Synthesis of Derivatives 9. In a 25 mL round-bottomed flask, 0.25 mmol of the respective triarylmethanol derivative was dissolved in 5 mL of $CDCl_3$. To the flask, trifluoroacetic acid (19 μL, 1 mmol, 4 equiv) was added using an automatic pipet. The initial, intense color of the resulting mixture disappeared within seconds. The subsequent thin layer chromatography of reaction mixture revealed total conversion of the substrate. The solvent was evaporated under reduced pressure and the crude product was purified using a column chromatography on silica gel (eluent: hexane/AcOEt, 95:5).

*2-(Diphenylmethyl)phenol (**9a**).*[27a] Isolated yield, 45 mg, 70% (eluent: hexane/AcOEt, 95:5), white solid. ^1H NMR (300 MHz, $CDCl_3$) δ 7.44−7.19 (m, 6H), 7.15 (dd, J = 9.9, 4.5 Hz, 5H), 6.94−6.68 (m, 3H), 5.74 (s, 1H), 4.65 (s, 1H). $^{13}C\{1H\}$ NMR (101 MHz, $CDCl_3$) δ 153.3, 142.5, 130.4, 129.3, 128.5, 127.9, 126.6, 120.7, 116.0, 50.7. ATR-IR 3513, 3060, 3022, 2923, 2851, 1595, 1489, 1446, 1325, 1266, 1173, 1086, 1042, 1030, 942, 921, 877, 814, 747, 725, 697 cm^{-1}. ESI HRMS m/z calcd for $C_{19}H_{16}ONa$ $[M + Na]^+$: 283.1093, found 283.1093. Mp 121−124 °C.

*2-(Bis(2-methoxyphenyl)methyl)phenol (**9b**).* Isolated yield, 63 mg, 79% (eluent: hexane/AcOEt, 95:5), white solid. ^1H NMR (400 MHz, $CDCl_3$) δ 7.24 (ddd, J = 8.4, 6.7, 2.4 Hz, 2H), 7.15−7.07 (m, 1H), 6.92−6.84 (m, 6H), 6.84−6.76 (m, 2H), 6.73 (dd, J = 7.6, 1.8 Hz, 1H), 6.26 (s, 1H), 4.90 (s, 1H), 3.71 (s, 6H). $^{13}C\{1H\}$ NMR (101 MHz, $CDCl_3$) δ 157.2, 153.5, 130.4, 129.8, 129.4, 127.8, 127.4, 120.4, 120.3, 115.8, 110.9, 55.7, 37.2. ATR-IR 3524, 3011, 2931, 2836, 1583, 1487, 1452, 1435, 1328, 1287, 1236, 1182, 1165, 1104, 1087, 1049, 1026, 938, 878, 854, 813, 790, 754, 651 cm^{-1}. ESI HRMS m/z calcd for $C_{21}H_{20}O_3Na$ $[M + Na]^+$: 343.1305, found 343.1303. Mp 155−156 °C.

General Procedure for in Situ Generation of Carbocations from Triarylmethanol Derivatives. In a 10 mL volumetric flask, 1 mg of triarylmethanol derivative was dissolved in 10 mL of dry MeCN. To the flask was added 20 μL of 0.1 M solution of trifluoroacetic acid (TFA) in MeCN containing 10% mol of trifluoroacetic anhydride (in relation to TFA) as an additive. The ECD spectra were measured directly after an addition of each portion of acid. The addition of acid was continued until there was no observable change in the ECD spectra or the analyzed compound decomposed.

The NMR spectra of in situ generated carbocations $\mathbf{6a}^+$ and $\mathbf{6b}^+$ were measured in dry $CDCl_3$ and with the use of TFA as acidifying agent. After dissolving respective triarylmethanol **6a** or **6b** in dry $CDCl_3$ and under an inert atmosphere, two equivalents of TFA were added in one portion. The NMR spectra were measured directly after addition of the acid.

https://dx.doi.org/10.1021/acs.joc.0c02289
J. Org. Chem. 2021, 86, 643−656

NMR Data for in Situ Generated Carbocations ***6a***$^+$ *and* ***6b***$^+$. **6a**$^+$: ^{1}H NMR (400 MHz, $CDCl_3$) δ 7.74−7.68 (dd, 1H), 7.66 (d, J = 9.1 Hz, 2H), 7.57 (d, J = 8.6 Hz, 2H), 7.29−7.21 (m, 5H), 7.19−7.10 (m, 3H), 7.08−7.03 (m, 2H), 6.98−6.92 (m, 2H), 5.22 (q, J = 6.4 Hz, 1H), 4.10 (d, J = 20.7 Hz, 6H), 1.21 (d, J = 6.4 Hz, 3H). ^{13}C{1H} NMR (101 MHz, $CDCl_3$) δ 192.8, 172.1, 159.7, 143.3, 140.8, 139.2, 138.2, 133.3, 133.2, 128.8, 128.7, 128.1, 125.3, 121.2, 114.8, 78.0, 57.0, 23.0.

6b$^+$: ^{1}H NMR (400 MHz, $CDCl_3$) δ 7.59−7.47 (m, 4H), 7.33 (m, J = 5.5, 4.3, 1.5 Hz, 5H), 7.29−7.21 (m, 4H), 7.08 (s, 2H), 6.96 (dt, J = 7.0, 1.7 Hz, 1H), 6.84 (d, J = 2.2 Hz, 1H), 5.29 (q, J = 6.4 Hz, 1H), 4.11 (s, 6H), 1.66 (d, J = 6.4 Hz, 3H). ^{13}C{1H} NMR (101 MHz, $CDCl_3$) δ 194.6, 171.9, 158.2, 144.0, 141.9, 139.8, 131.2, 130.3, 128.9, 128.5, 127.9, 126.3, 125.3, 123.6, 116.5, 76.8, 57.1, 24.5.

■ ASSOCIATED CONTENT

Supporting Information

The Supporting Information is available free of charge at https://pubs.acs.org/doi/10.1021/acs.joc.0c02289.

Calculation details, X-ray crystallography details, total energies, percentage populations and structures of all calculated low-energy conformers, calculated UV and ECD spectra, copies of the UV and ECD spectra of **3**−**7** measured in acetonitrile and acidified acetonitrile, ^{1}H and ^{13}C{1H} NMR spectra of all synthesized new compounds, and the Cartesian coordinates for all calculated structures (PDF)

FAIR data, including the primary NMR FID files, for compounds **2**−**9** and for in situ generated carbocations **6a**$^+$ and **6b**$^+$ (ZIP)

Accession Codes

CCDC 2002970−2002974 contain the supplementary crystallographic data for this paper. These data can be obtained free of charge via www.ccdc.cam.ac.uk/data_request/cif, or by emailing data_request@ccdc.cam.ac.uk, or by contacting The Cambridge Crystallographic Data Centre, 12 Union Road, Cambridge CB2 1EZ, UK; fax: +44 1223 336033.

■ AUTHOR INFORMATION

Corresponding Authors

Bartosz Stasiak − *Faculty of Chemistry, Adam Mickiewicz University, 61 614 Poznań, Poland;* orcid.org/0000-0001-6884-3256; Email: bartosz.stasiak@amu.edu.pl

Marcin Kwit − *Faculty of Chemistry and Centre for Advanced Technologies, Adam Mickiewicz University, 61 614 Poznań, Poland;* orcid.org/0000-0002-7830-4560; Email: marcin.kwit@amu.edu.pl

Author

Agnieszka Czapik − *Faculty of Chemistry, Adam Mickiewicz University, 61 614 Poznań, Poland*

Complete contact information is available at: https://pubs.acs.org/10.1021/acs.joc.0c02289

Notes

The authors declare no competing financial interest.

■ ACKNOWLEDGMENTS

This work was supported by a research grant from National Science Center (NCN) Poland, Grant UMO-2016/21/B/ST5/00100. All calculations were performed at Poznan Supercomputing and Networking Centre.

■ DEDICATION

Dedicated to Prof. Bogdan Marciniec on the occasion of his 80th birthday.

■ REFERENCES

(1) (a) Greene, T. W.; Wats, P. G. M. *Protective Groups in Organic Synthesis*; Wiley: New York, 2006. (b) Kocienski, P. J. *Protective Groups*, 3rd ed.; Georg Thieme: Stuttgart, 2003.

(2) Akazome, M. In *Advances in Organic Crystal Chemistry*; Tamura, R., Miyata, M., Eds.; Springer: Berlin, 2015; Chapter 23, p 463.

(3) See, for example: (a) Duong, A.; Lévesque, A.; Homand, C.; Maris, T.; Wuest, J. D. Controlling Molecular Organization by Using Phenyl Embraces of Multiple Trityl Groups. *J. Org. Chem.* **2020**, *85*, 4026−4035. (b) Dominguez, Z.; Dang, H.; Strouse, M. J.; Garcia-Garibay, M. A. Molecular "Compasses" and "Gyroscopes". I. Expedient Synthesis and Solid State Dynamics of an Open Rotor with a Bis(triarylmethyl) Frame. *J. Am. Chem. Soc.* **2002**, *124*, 2398−2399. (c) Stopin, A.; Garcia-Garibay, M. A. Crystals and Aggregates of a Molecular Tetrarotor with Multiple Trityl Embraces Derived from Tetraphenyladamantane. *Cryst. Growth Des.* **2012**, *12*, 3792−3798. (d) Tohnai, N.; Mizobe, Y.; Doi, M.; Sukata, S.; Hinoue, T.; Yuge, T.; Hisaki, I.; Matsukawa, Y.; Miyata, M. Well-designed supramolecular clusters comprising triphenylmethylamine and various sulfonic acids. *Angew. Chem., Int. Ed.* **2007**, *46*, 2220−2223. (e) Pantos, G. D.; Wietor, J.-L.; Sanders, J. K. M. Filling Helical Nanotubes with C_{60}. *Angew. Chem., Int. Ed.* **2007**, *46*, 2238−2240. (f) Karlen, S. D.; Garcia-Garibay, M. A. Amphidynamic Crystals: Structural Blueprints for Molecular Machines. *Top. Curr. Chem.* **2005**, *262*, 179−227. (g) West, K. R.; Bake, K. D.; Otto, S. Dynamic Combinatorial Libraries of Disulfide Cages in Water. *Org. Lett.* **2005**, *7*, 2615−2618. (h) Charlier, N.; Driesschaert, B.; Wauthoz, N.; Beghein, N.; Préat, V.; Amighi, K.; Marchand-Brynaert, J.; Gallez, B. Nano-emulsions of fluorinated trityl radicals as sensors for EPR oximetry. *J. Magn. Reson.* **2009**, *197*, 176−180. (i) Dattler, D.; Fuks, G.; Heiser, J.; Moulin, E.; Perrot, A.; Yao, X.; Giuseppone, N. Design of Collective Motions from Synthetic Molecular Switches, Rotors, and Motors. *Chem. Rev.* **2020**, *120*, 310−433.

(4) See, for example: (a) Kaan, H. Y.; Weiss, J.; Menger, D.; Ulaganathan, V.; Tkocz, K.; Laggner, C.; Popowycz, F.; Joseph, B.; Kozielski, F. Structure−Activity Relationship and Multidrug Resistance Study of New *S*-trityl-l-Cysteine Derivatives As Inhibitors of Eg5. *J. Med. Chem.* **2011**, *54*, 1576−1586. (b) Kozielski, F.; Skoufias, D. A.; Indorato, R. L.; Saoudi, Y.; Jungblut, P. R.; Hustoft, H. K.; Strozynski, M.; Thiede, B. Proteome analysis of apoptosis signaling by *S*-trityl-l-cysteine, a potent reversible inhibitor of human mitotic kinesin Eg5. *Proteomics* **2008**, *8*, 289−300. (c) Radwan, M. O.; Ciftci, H. I.; Ali, T. F. S.; Koga, R.; Tateishi, H.; Nakata, A.; Ito, A.; Yoshida, M.; Fujita, M.; Otsuka, M. Structure activity study of *S*-trityl-cysteamine dimethylaminopyridine derivatives as SIRT2 inhibitors: Improvement of SIRT2 binding and inhibition. *Bioorg. Med. Chem. Lett.* **2020**, *30*, No. 127458. (d) Skoufias, D. A.; DeBonis, S.; Saoudi, Y.; Lebeau, L.; Crevel, I.; Cross, R.; Wade, R. H.; Hackney, D.; Kozielski, F. *S*-trityl-l-cysteine is a reversible, tight binding inhibitor of the human kinesin Eg5 that specifically blocks mitotic progression. *J. Biol. Chem.* **2006**, *281*, 17559−17569. (e) Zee-Cheng, K. Y.; Cheng, C. C. Structural modification of *S*-trityl-l-cysteine. Preparation of some *S*-(substituted trityl)-l-cysteines and dipeptides of *S*-trityl-l-cysteine. *J. Med. Chem.* **1972**, *15*, 13−16.

(5) See reviews: (a) Olah, G. A. My Search for Carbocations and Their Role in Chemistry (Nobel Lecture). *Angew. Chem., Int. Ed. Engl.* **1995**, *34*, 1393−1405. (b) Olah, G. A. 100 Years of Carbocations and Their Significance in Chemistry. *J. Org. Chem.* **2001**, *66*, 5943−5957. (c) Nair, V.; Thomas, S.; Mathew, S. C.; Abhilash, K. G. Recent advances in the chemistry of triaryl- and triheteroarylmethanes. *Tetrahedron* **2006**, *62*, 6731−6747.

(6) (a) Naidu, V. R.; Ni, S.; Franzén, J. The Carbocation: A Forgotten Lewis Acid Catalyst. *ChemCatChem* **2015**, *7*, 1896−1905. (b) Courant, T.; Lombard, M.; Boyarskaya, D. V.; Neuville, L.;

Masson, G. Tritylium assisted iodine catalysis for the synthesis of unsymmetrical triarylmethanes. *Org. Biomol. Chem.* **2020**, *18*, 6502−6508. (c) Ni, S.; El Remaily, A. E. A. M. A. A.; Franzén, J. Carbocation Catalyzed Bromination of Alkyl Arenes, a Chemoselective sp^3 vs. sp^2 C-H functionalization. *Adv. Synth. Catal.* **2018**, *360*, 4197−4204. (d) Ni, S.; Franzén, J. Carbocation catalysed ring closing aldehyde−olefin metathesis. *Chem. Commun.* **2018**, *54*, 12982−12985. (e) Kennington, S. C. D.; Ferre, M.; Romo, J. M.; Romea, P.; Urpí, F.; Font-Bardia, M. Diastereoselective and Catalytic α-Alkylation of Chiral *N*-Acyl Thiazolidinethiones with Stable Carbocationic Salts. *J. Org. Chem.* **2017**, *82*, 6426−6433. (f) Nomoto, Y.; Horinouchi, R.; Nishiyama, N.; Nakano, K.; Ichikawa, Y.; Kotsuki, H. Trityl Cation Catalyzed Intramolecular Carbonyl-Ene Cyclization and [2 + 2] Cycloaddition. *Synlett* **2017**, *28*, 265−269. (g) El Remaily, M. A. E. A. A. A.; Naidu, V. R.; Ni, S.; Franzén, J. Carbocation Catalysis: Oxa-Diels−Alder Reactions of Unactivated Aldehydes and Simple Dienes. *Eur. J. Org. Chem.* **2015**, *2015*, 6610−6614. (h) Bah, J.; Franzén, J. Carbocations as Lewis Acid Catalysts in Diels−Alder and Michael Addition Reactions. *Chem. - Eur. J.* **2014**, *20*, 1066−1072. (i) Chen, Y.-L.; Barton, T. J. Trityl Cation Catalyzed Intramolecular Cyclizations of Saturated and Unsaturated γ- and δ-Alkoxysilyl Hydrides. *Organometallics* **1987**, *6*, 2590−2592.

(7) Chen, C.-T.; Chao, S.-D.; Yen, K.-C.; Chen, C.-H.; Chou, I.-C.; Hon, S.-W. Chiral Triarylcarbenium Ions in Asymmetri Mukaiyama Aldol Additions. *J. Am. Chem. Soc.* **1997**, *119*, 11341−11342.

(8) Lv, J.; Zhang, Q.; Zhong, X.; Luo, S. Asymmetric Latent Carbocation Catalysis with Chiral Trityl Phosphate. *J. Am. Chem. Soc.* **2015**, *137*, 15576−15583.

(9) (a) Zhang, Q.; Lv, J.; Luo, S. Enantioselective Diels−Alder reaction of anthracene by chiral tritylium catalysis. *Beilstein J. Org. Chem.* **2019**, *15*, 1304−1312. (b) Pommerening, P.; Mohr, J.; Friebel, J.; Oestreich, M. Synthesis of a Chiral Borate Counteranion, Its Trityl Salt, and Application Thereof in Lewis-Acid Catalysis. *Eur. J. Org. Chem.* **2017**, *2017*, 2312−2316. (c) Ni, S.; Naidu, V. R.; Franzén, J. Chiral Anion Directed Asymmetric Carbocation-Catalyzed Diels−Alder Reactions. *Eur. J. Org. Chem.* **2016**, *2016*, 1708−1713.

(10) (a) Blount, J. F.; Finocchiaro, P.; Gust, D.; Mislow, K. Conformational analysis of triarylboranes. *J. Am. Chem. Soc.* **1973**, *95*, 7019−7029. (b) Boettcher, R. J.; Gust, D.; Mislow, K. Dynamic stereochemistry of triarylsilanes. *J. Am. Chem. Soc.* **1973**, *95*, 7157−7158. (c) Finocchiaro, P.; Gust, D.; Mislow, K. Separation of conformational stereoisomers in a triarylmethane. A Novel Type of Stereoisomerism. *J. Am. Chem. Soc.* **1973**, *95*, 8172−8173. (d) Kawada, Y.; Iwamura, H. Phase isomerism in gear-shaped molecules. *Tetrahedron Lett.* **1981**, *22*, 1533−1536. (e) Kawada, Y.; Iwamura, H.; Okamoto, Y.; Yuki, H. Stereoisomerism in molecular bevel-gears. Optical resolution of the dl isomers of bis(2- and 3-chloro-9-triptycyl)methanes and ethers. *Tetrahedron Lett.* **1983**, *24*, 791−794. (f) Iwamura, H. Molecular design of correlated internal rotation. *J. Mol. Struct.* **1985**, *126*, 401−412.

(11) (a) Mislow, K. Stereochemical consequences of correlated rotation in molecular propellers. *Acc. Chem. Res.* **1976**, *9*, 26−33. (b) Iwamura, H.; Mislow, K. Stereochemical consequences of dynamic gearing. *Acc. Chem. Res.* **1988**, *21*, 175−182.

(12) Wolf, C. *Dynamic Stereochemistry of Chiral Compounds: Principles and Applications*; Royal Society of Chemistry: Cambridge, 2008.

(13) Ściebura, J.; Skowronek, P.; Gawroński, J. Trityl Ethers: Molecular Bevel Gears Reporting Chirality through Circular Dichroism Spectra. *Angew. Chem., Int. Ed.* **2009**, *48*, 7069−7072.

(14) See, for example: (a) Wang, L.; Zhang, T.; Redden, B. K.; Sheppard, C. I.; Clark, R. W.; Smith, M. D.; Wiskur, S. L. Understanding Internal Chirality Induction of Triarylsilyl Ethers Formed from Enantiopure Alcohols. *J. Org. Chem.* **2016**, *81*, 8187. (b) Skowronek, P.; Ścianowski, J.; Pacuła, A. J.; Gawroński, J. Chirality transfer through sulfur or selenium to chiral propellers. *RSC Adv.* **2015**, *5*, 69441−69444. (c) Prusinowska, N.; Bendzińska-Berus, W.; Jelecki, M.; Rychlewska, U.; Kwit, M. Triphenylacetic Acid Amides: Molecular Propellers with Induced Chirality. *Eur. J. Org. Chem.* **2015**, *2015*, 738−749. (d) Ściebura, J.; Gawroński, J. Double Chirality Transmission in Trityl Amines: Sensing Molecular Dynamic Stereochemistry by Circular Dichroism and DFT Calculations. *Chem. - Eur. J.* **2011**, *17*, 13138−13141.

(15) (a) Bendzińska-Berus, W.; Jelecki, M.; Kwit, M.; Rychlewska, U. Transfer of chirality in *N*-triphenylacetylamino acids and chiral derivatives of *N*-triphenylacetyl Gly−Gly dipeptide and control of their assembly with steric constraints. *CrystEngComm* **2019**, *21*, 3420−3430. (b) Prusinowska, N.; Czapik, A.; Wojciechowska, M.; Kwit, M. Dynamic optical activity induction in the *N*-alkyl-*N*′-trityl ureas and thioureas. *Org. Biomol. Chem.* **2019**, *17*, 7782−7793. See also references cited therein.

(16) (a) Mayorga Burrezo, P.; Jimenez, V. G.; Blasi, D.; Ratera, I.; Campana, A. G.; Veciana, J. Organic Free Radicals as Circularly Polarized Luminescence Emitters. *Angew. Chem., Int. Ed.* **2019**, *58*, 16282−16288. (b) Li, Y.; Zhai, W.; Liao, Y.; Nie, J.; Han, G.; Song, Y.; Li, S.; Hou, J.; Liu, Y. Synthesis of Central Chirality-Containing Triarylmethanols and Triarylmethyl Radicals with Extraordinarily Stable Configurations. *J. Org. Chem.* **2019**, *84*, 11774−11782. (c) Zhai, W.; Feng, Y.; Liu, H.; Rockenbauer, A.; Mance, D.; Li, S.; Song, Y.; Baldus, M.; Liu, Y. Diastereoisomers of L-proline-linked tritylnitroxide biradicals: synthesis and effect of chiral configurations on exchange interactions. *Chem. Sci.* **2018**, *9*, 4381−4391. (d) Driesschaert, B.; Robiette, R.; Lucaccioni, F.; Gallez, B.; Marchand-Brynaert, J. Chiral properties of tetrathiatriarylmethyl spin probes. *Chem. Commun.* **2011**, *47*, 4793−4795.

(17) (a) Gawroński, J.; Koput, J.; Wierzbicki, A. On the Induced Optical Activity of Triphenylmethane Dyes. *Z. Naturforsch., A: Phys. Sci.* **1986**, *41a*, 1245−1249. (b) Murr, B. L.; Feller, L. W. The Optical Rotation of an Asymmetric Carbonium Ion and Microscopic Reversibility in Carbonium Ion Reactions. *J. Am. Chem. Soc.* **1968**, *90*, 2966−2967.

(18) Mori, T.; Inoue, Y. Chiral Organic Radical Cation and Dication. A Reversible Chiroptical Redox Switch Based on Stepwise Transformation of Optically Active Tetrakis(p-alkoxyphenyl)-ethylenes to Radical Cations and Dications. *J. Phys. Chem. A* **2005**, *109*, 2728−2740.

(19) (a) Ishigaki, Y.; Iwai, T.; Hayashi, Y.; Nagaki, A.; Katoono, R.; Fujiwara, K.; Yoshida, J.; Suzuki, T. Transmission of Point Chirality to Axial Chirality for Strong Circular Dichroism in Triarylmethylium-*o*,*o*-dimers. *Synlett* **2018**, *29*, 2147−2154. (b) Suzuki, T.; Iwai, T.; Ohta, E.; Kawai, H.; Fujiwara, K. Electrochiroptical systems based on biphenyl-2,20-diyl-type dicationic dyes: strong chiroptical signals through the transmission of point chirality to axial chirality. *Tetrahedron Lett.* **2007**, *48*, 3599−3603.

(20) Horn, M.; Mayr, H. A comprehensive view on stabilities and reactivities of triarylmethyl cations (tritylium ions). *J. Phys. Org. Chem.* **2012**, *25*, No. 979.

(21) Following the request of one of the reviewers, we have measured the ECD spectra of racemic sample of **3a**. As expected, the racemate did not exhibit any Cotton effects (see Figure S69).

(22) (a) Lightner, D. A.; Gurst, J. E. *Organic conformational analysis and stereochemistry from circular dichroism spectroscopy*; Wiley-VCH, New York, 2000. (b) Pescitelli, G.; Di Bari, L.; Berova, N. Conformational aspects in the studies of organic compounds by electronic circular dichroism. *Chem. Soc. Rev.* **2011**, *40*, 4603−4625. (c) Grauso, L.; Teta, R.; Esposito, G.; Menna, M.; Mangoni, A. Computational prediction of chiroptical properties in structure elucidation of natural products. *Nat. Prod. Rep.* **2019**, *36*, 1005−1030. (d) Pescitelli, G.; Bruhn, T. Good computational practice in the assignment of absolute configurations by TDDFT calculations of ECD spectra. *Chirality* **2016**, *28*, 466−474. (e) Autschbach, J. Computing chiroptical properties with first-principles theoretical methods: background and illustrative examples. *Chirality* **2009**, *21*, E116−E152.

(23) IEFPCM/TD-CAM-B3LYP/6-311++G(2d,2p)//IEFPCM/B3LYP/6-311++G(d,p) method as implemented in Gaussian software:Frisch, M. J.; Trucks, G. W.; Schlegel, H. B.; Scuseria, G. E.; Robb, M. A.; Cheeseman, J. R.; Scalmani, G.; Barone, V.;

https://dx.doi.org/10.1021/acs.joc.0c02289
J. Org. Chem. 2021, 86, 643−656

Mennucci, B.; Petersson, G. A.; Nakatsuji, H.; Caricato, M.; Li, X.; Hratchian, H. P.; Izmaylov, A. F.; Bloino, J.; Zheng, G.; Sonnenberg, J. L.; Hada, M.; Ehara, M.; Toyota, K.; Fukuda, R.; Hasegawa, J.; Ishida, M.; Nakajima, T.; Honda, Y.; Kitao, O.; Nakai, H.; Vreven, T.; Montgomery, J. A., Jr.; Peralta, J. E.; Ogliaro, F.; Bearpark, M. J.; Heyd, J.; Brothers, E. N.; Kudin, K. N.; Staroverov, V. N.; Kobayashi, R.; Normand, J.; Raghavachari, K.; Rendell, A. P.; Burant, J. C.; Iyengar, S. S.; Tomasi, J.; Cossi, M.; Rega, N.; Millam, N. J.; Klene, M.; Knox, J. E.; Cross, J. B.; Bakken, V.; Adamo, C.; Jaramillo, J.; Gomperts, R.; Stratmann, R. E.; Yazyev, O.; Austin, A. J.; Cammi, R.; Pomelli, C.; Ochterski, J. W.; Martin, R. L.; Morokuma, K.; Zakrzewski, V. G.; Voth, G. A.; Salvador, P.; Dannenberg, J. J.; Dapprich, S.; Daniels, A. D.; Farkas, O.; Foresman, J. B.; Ortiz, J. V.; Cioslowski, J.; Fox, D. J. Gaussian 09, revision D.01; Gaussian, Inc.: Wallingford, CT, 2009.

(24) (a) Becke, A. D. Density-Functional Thermochemistry. III. The Role of Exact Exchange. *J. Chem. Phys.* **1993**, *98*, No. 5648. (b) Lee, C.; Yang, W.; Parr, R. G. Development of the Colle-Salvetti Correlation-Energy Formula into a Functional of the Electron Density. *Phys. Rev. B: Condens. Matter Mater. Phys.* **1988**, *37*, 785−789. (c) Yanai, T.; Tew, D.; Handy, N. A new hybrid exchange-correlation functional using the Coulomb-attenuating method (CAM-B3LYP). *Chem. Phys. Lett.* **2004**, *393*, 51−57.

(25) The term quasi-symmetrical is related to the structure of the triphenyl moiety only, without considering the presence of substituents, and rather describes the same sense of the twist not the same numerical values of the angles. In fact, the compounds studied here are asymmetric without exception (of C_1 symmetry).

(26) Górczyńska, S.; Brzdonkiewicz, A.; Jelecki, M.; Czapik, A.; Stasiak, B.; Kwit, M. Trityl-containing alcohols − an efficient chirality transmission process from inductor to the stereodynamic propeller and their solid-state structural diversity. *Molecules* **2020**, *25*, No. 707.

(27) (a) Starnes, W. H., Jr. Fragmentation of Some Trityl Compounds by Means of Hydride Transfer. A Reinvestigation of an Unusual Reaction Reported by Gomberg. *J. Org. Chem.* **1971**, *36*, 2508−2516. (b) Doyle, M. P.; DeBruyn, D. J.; Scholten, D. J. The Disproportionation of Trityl Alkyl Ethers. The Synthesis of Aldehydes and Ketones in a Cationic Chain Reaction Involving Hydride Transfer. *J. Org. Chem.* **1973**, *38*, 625−626.

(28) (a) Lomas, J. S.; Vaissermann, J. 1,4-Hydride shifts in *ortho*-alkyl-substituted di(1-adamantyl)benzyl cations: an NMR spectroscopic and X-ray crystallographic study. *J. Chem. Soc., Perkin Trans. 2* **1996**, 1831−1836. (b) Lomas, J. S.; Vauthier, E.; Vaissermann, J. Trifluoroacetylation and ionic hydrogenation of [2-(3-alkoxythienyl)]di(1-adamantyl)methanols. *J. Chem. Soc. Perkin. Trans. 2* **2000**, 1399−1408. (c) Lomas, J. S.; Vauthier, E. Hydrosilane reduction and 1,5-hydride transfer in the [2-(3-ethoxythienyl)]di(1-adamantyl)methyl cation. *J. Chem. Soc., Perkin Trans. 2* **2000**, 417−418.

(29) See, for example: (a) Hojo, M.; Ueda, T.; Yamasaki, M.; Inoue, A.; Tokita, S.; Yanagita, M. ^{1}H and ^{13}C NMR Detection of the Carbocations or Zwitterions from Rhodamine B Base, a Fluoran-Based Black Color Former, Trityl Benzoate, and Methoxy-Substituted Trityl Chlorides in the Presence of Alkali Metal or Alkaline Earth Metal Perchlorates in Acetonitrile Solution. *Bull. Chem. Soc. Jpn.* **2002**, *75*, 1569−1576. (b) Canle L., M.; Clegg, W.; Demirtas, I.; Elsegood, M. R. J.; Maskill, H. Preparations, X-ray crystal structure determinations, and base strength measurements of substituted tritylamines. *J. Chem. Soc. Perkin Trans. 2* **2000**, *8*, 85−92.

(30) Due to the significant dilution of the sample (below 10^{-6} mol L^{-1}), further measurements were difficult to perform.

(31) Newcomb, M.; Varick, T. R.; Goh, S.-H. Mechanism of Reduction of Trityl Halides by Lithium Dialkylamide Bases. *J. Am. Chem. Soc.* **1990**, *112*, 5186−5193.

(32) Czapik, A.; Jelecki, M.; Kwit, M. Chiral Cocrystal Solid Solutions, Molecular Complexes, and Salts of *N*-Triphenylacetyl-l-Tyrosine and Diamines. *Int. J. Mol. Sci.* **2019**, *20*, No. 5004.

(33) Jacques, J.; Collet, A.; Wilen, S. *Enantiomers, Racemates and Resolutions*; Wiley: New York, 1981.

(34) To the best of our knowledge, similar systems were studied only as a student project:Grau, A. A. P. *Synthesis and Application of Chiral Carbocations*; KTH Royal Institute Of Technology: Stockholm, Sweden, 2015.

https://dx.doi.org/10.1021/acs.joc.0c02289
J. Org. Chem. 2021, 86, 643−656